Optimising DNA-Coated Gold Nanoparticles to Enrich Skeletal Stem Cells from Human Bone Marrow Samples

S.A. Lanham[1*§], M. Xavier[1*], M.E. Kyriazi[2], K. Alexaki[2], A.H. El-Sagheer[3], T. Brown[3], A.G. Kanaras[2§] and R.O.C. Oreffo[1§].

* S.A. Lanham and M. Xavier contributed equally to this work.

[1] Bone and Joint Research Group, Centre for Human Development, Stem Cells and Regeneration, Human Development and Health, Institute of Developmental Sciences, Faculty of Medicine, University of Southampton, Southampton, SO16 6YD, UK

[2] Physics and Astronomy, Faculty of Physical Sciences and Engineering, University of Southampton, Southampton SO17 1BJ, UK

[3] Department of Chemistry, University of Oxford, Chemistry Research Laboratory, 12 Mansfield Road, Oxford OX1 3TA, UK

Article Type: Original Article.

Running Title: Nanoprobes to Isolate Human Bone Marrow Cells

Author's Email:	S. Lanham	S.A.Lanham@soton.ac.uk
	M. Xavier	J.Xavier@soton.ac.uk
	M.E. Kyriazi	M.Kyriazi@soton.ac.uk
	K. Alexaki	K.Alexaki@soton.ac.uk
	A.H. El-Sagheer	afaf.el-sagheer@chem.ox.ac.uk
	T. Brown	tom.brown@chem.ox.ac.uk
	A.G. Kanaras	A.Kanaras@soton.ac.uk
	R.O.C. Oreffo	roco@soton.ac.uk

[§]Corresponding Authors: Stuart Lanham, Richard Oreffo or Antonios Kanaras

Fax: +44 2381 205255

Email: S.A.Lanham@soton.ac.uk or roco@soton.ac.uk or A.Kanaras@soton.ac.uk

Abstract Word Count: 152

Manuscript Word Count: 4323

Number of Figures: 11

Number of Tables: 2

Keywords: Nanoprobe, human bone marrow

Abstract

There is a wealth of data indicating human bone marrow derived stromal cells (HBMSCs) contain the skeletal stem cell (SSC) with the potential to differentiate along the osteogenic, adipogenic and chondrogenic lineages leading to significant interest as potential clinical therapies. However, despite these advances, current methods to isolate skeletal stem cells (SSCs) from human tissues are difficult as no single specific marker has been identified. Hence, limited understanding of SSC fate, immuno-phenotype and simple selection criteria proved to be limiting factors in the widespread clinical application of these cells. While a range of cell surface markers can enrich for SSCs, none of the proposed markers, alone, isolate single cells with the ability to form bone, cartilage, and adipose tissue in humans. In this work, we have developed a methodology to use oligonucleotide-coated gold nanoparticles to identify cells in human bone marrow displaying specific mRNA signatures to isolate and enrich for the SSCs.

Introduction

The fate of cells in culture, tissues, and organisms can be followed by a variety of techniques from fluorescently-labelled antibodies to application of quantum dots, although cell phenotype information is typically limited to cell surface epitopes [1]. The detection of a specific mRNA responsible for the expression of a certain protein can be used to determine and characterise the phenotype of the cell. However, traditional methods to quantitatively analyse expression of specific mRNAs such as *in-situ* hybridisation, northern blot, or quantitative-PCR require cell fixation or lysis to isolate the RNA, resulting in loss of the cells for further experiments.

Over the last few years, gold nanoparticles (AuNPs) have come to the fore in biomedicine given their ease of synthesis, tunability and potential for surface ligand functionalisation with, for example, oligonucleotides. These oligonucleotide functionalised AuNPS display enhanced stability, excellent cell uptake and a degree of resistance to enzyme degradation conferring additional attractive drug delivery properties. Furthermore, they can be tailored to enhance selectivity and specificity towards the detection of intracellular targets such as RNA. Recently, Mirkin's group reported that gold nanoparticles coated with a dense shell of synthetic oligonucleotides showed excellent biocompatibility, bio-stability and uptake by a large range of different cell types, without the requirement for additional co- carriers [2] for the detection of different RNA targets. We developed this work further and have recently designed nanoprobes which consist of DNA sense strands, bearing a 5′ (FAM) fluorophore, attached to a gold nanoparticle surface. These were partially hybridised to short oligonucleotide complements, termed flare strands, with an additional dye at their 3′ end [3]. Critically, the sequence of the DNA sense strand determines the specificity to which mRNA the nanoprobe will bind. When the nanoprobe is fully assembled, the fluorescence of all fluorophores is quenched, due to the close proximity to the AuNP surface [4]. However, once the target mRNA binds to the corresponding nanoprobe sense sequence, the resulting displacement of the flare can be detected as an increase in fluorescence at the specific wavelength of the fluorophore [5]. Such a tailored construct ensures the fluorophore on the sense strand in this design acts as a reporter, whilst the FAM signal from the sense strand acts as a DNA degradation control, with the fluorophore being released, and detectable, only if the DNA is degraded by nucleases.

The capacity of bone to regenerate is evidence of the presence of a stem cell in bone and while this regenerative capacity has long been recognized, the *in vivo* identity of the skeletal population has only recently been confirmed [6-8]. There is a wealth of data indicating human bone marrow derived stromal cells (HBMSCs) contain the skeletal stem cell (SSC) with the potential to differentiate along the osteogenic, adipogenic and chondrogenic lineages leading to significant interest as potential clinical therapies [9]. However, despite these advances, current methods to isolate skeletal stem cells (SSCs) from human tissues are difficult as no single specific marker has been identified. Thus, to date, there remains limited understanding of SSC fate, immuno-phenotype and simple selection criteria all of which have proved to be limiting factors in the widespread clinical application of these cells [10]. While a range of cell

surface markers can enrich for SSCs [6, 11, 12], none of the proposed markers, alone, isolate single cells with the ability to form bone, cartilage, and adipose tissue in humans.
In this work, we use the aforementioned oligonucleotide coated gold nanoparticles to identify cells in human bone marrow displaying specific mRNA signatures which could be used to isolate and enrich for the SSCs. To achieve this objective, the current studies have developed and designed protocols which would enable detection without affecting long term cell viability.

Methods

Cell Culture

MG-63 and Saos-2 human osteosarcoma cells were cultured in DMEM (Lonza, Slough, UK) and α-MEM, respectively, supplemented with 10% FBS, 100 U ml^{-1} penicillin and 100 µg ml^{-1} streptomycin, and maintained at 37°C and 5% CO_2.
Bone marrow samples were obtained from haematologically healthy patients undergoing hip replacement surgery with local ethics committee approval (LREC194/99/1 and 18/NW/0231 and 210/01). Bone marrow was first washed in α-MEM medium, then passed through a 70-µm cell strainer and subjected to density centrifugation using Lymphoprep™ (Lonza). The buffy coat layer, containing bone marrow mononuclear cells was washed in basal medium (α-MEM containing 10% FBS and 100 U ml^{-1} penicillin and 100 µg ml^{-1} streptomycin; Lonza).

DNA-Gold Nanoparticles for mRNA Detection

DNA-Gold Nanoparticles for mRNA Detection were manufactured as previously detailed [13]. The sequences used are detailed in Table 1. All sense strands contained FAM at the 5' end and a thiol at the 3' end. All flare strands contained Cy5 at the 5' end. For adherent cells, the nanoprobes were added to the medium to the final concentration indicated. If required, cells in suspension were first stained for Stro-1 (see below). The particles were then added to the cell suspension (at 10^6 cells per ml) to the required final concentration and for the appropriate contact time. Cells were then washed in basal medium and then resuspended in FACS solution (0.5% BSA, 2mM EDTA in 1x PBS) prior to FACS analysis.

Microscopy

Cells were cultured at 37°C in 5% CO_2 in 24 well plates and imaged using a Zeiss Axiovert 200 inverted microscope with an Axiocam MR camera for fluorescent imaging and Axiovert HR camera for white light imaging operated by Zeiss Axiovision software version 4.7.
For cellular necrosis, the RealTime-Glo Annexin V Apoptosis and Necrosis Assay (Promega, Southampton, UK) was used according to manufacturer's instructions. Necrosis was detected using the FITC channel settings on the microscope.

FACS

Cell suspensions were stained with Stro-1 antibody from an in-house generated mouse hybridoma. Following incubation with primary antibody and washing, cells were incubated with fluorescent AlexaFluor 488–conjugated anti-mouse IgM secondary antibody (Invitrogen, ThermoFisher Scientific, Loughborough, UK). Nanoprobes were then added to the cells as detailed above. The FACS Aria cytometer (Becton Dickinson, Wokingham, UK) was used to acquire 20000 cells with data analysed using the FlowJo software version 10.6.1.

Cell Viability

Cells were cultured in white opaque 96 well tissue culture plates (ThermoFisher Scientific) for the appropriate time. Cells were subsequently washed with PBS and lysed using the

CellTiter-Glo kit (Promega) according to the manufacturer's instructions. The plate was read in a GloMax Discover Multimode plate reader (Promega) using the predefined kit settings.

Colony Forming Units-Fibroblast (CFU-F) Assay

The FACS Aria was used to collect nanoprobe positive and nanoprobe negative cells from human bone marrow samples. Cells were gated for monocytes, single cells, and Cy5 fluorescence. Positive samples were deemed to be the top 15% of Cy5 fluorescent cells and negative samples were deemed to be the lower 15% of Cy5 cells collected.

Cy5 positive and negative cells were collected by FACS sorting. Ten thousand cells were placed into each well of 6-well tissue culture plates. Cells were grown for 14 days, with a medium change after 7 days. On day 14, wells were washed with PBS and then fixed with 95% ethanol for 10 minutes. The wells were then air dried and 1ml 0.05% crystal violet solution added to each well for 1 minute. The wells were then washed twice with distilled water and the number of visible colonies determined by eye.

Gene Expression

RNA was extracted from samples using ReliaPrep RNA Cell MiniPrep system kit (Promega) according to manufacturer's instructions, and cDNA produced from the same volume of RNA solution for each sample using a Taqman reverse transcription kit with random hexamers (Applied Biosystems) following manufacturer's instructions.

Quantitative PCR

Relative quantification of gene expression was performed with an ABI Prism 7500 detection system (Applied Biosystems). The 20 µl reaction mixture was prepared, containing 1 µl of complementary DNA, 10 µl of GoTaq qPCR Master Mix (Promega, Southampton, UK), and 250 nM of each primer. Thermal cycler conditions consisted of an initial activation step at 95 °C for 10 min, followed by a 2-step PCR program of 95 °C for 15 s and 60 °C for 60 s for 40 cycles. The primers used for qPCR are shown in table 2. Relative gene expression levels were determined based on threshold (CT) value.

Longitudinal Cy5 Detection

Two hundred microlitres of MG-63 cells at various concentrations were added to wells of a qPCR plate. The wells contained nanoprobes specific for scrambled, *RUNX2*, or *Osteocalcin* to give a final concentration of 0.2 nM after the cells were added. The plates were then sealed and incubated continuously at 37 °C with the Cy5 signal collected every 10 minutes for 15 hours in an ABI Prism 7500 detection system (Applied Biosystems).

Statistics

Wilcoxon-Mann-Whitney statistical analysis and ANOVA were performed where appropriate using the SPSS for Windows program version 23 (IBM Corp, Portsmouth, Hampshire, UK). All experiments were completed at least three times and data are presented as mean ± 95% confidence limits. Significance was determined with a p-level of 0.05 or lower.

Results

Nanoprobe in human skeletal cell lines.

In order to determine if the Cy5 signal from the nanoprobes was only transient, *Vimentin* nanoprobes at different final concentrations (0.2 nM, 1 nM, and 6.25 nM) were added to the adherent human cell lines MG-63 and Saos-2, which express vimentin mRNA. After 9 days incubation with the nanoprobes (media change without nanoprobes after 4 and 7 days), the Cy5 flare strand was still detectable and visible within cells (Figure 1A). Critically, there was no evidence of FAM dye (Figure 1B) indicating the nanoprobe particles were not degraded.

Cell Viability was Related to Nanoprobe Exposure Time and Concentration.

After 9 days exposure to nanoprobes, MG-63 and Saos-2 cell growth was lower than expected, with the skeletal populations far from confluent (Figure 1). As a consequence, the toxicity of the nanoprobes was tested. *Vimentin* nanoprobes were added to the adherent human cell lines MG-63 and Saos-2 at different final concentrations (0.2 nM, 1 nM, and 6.25 nM). RealTime-Glo Annexin V Apoptosis and Necrosis Assay reagents were added to detect cell necrosis using photomicroscopy. Cells were healthy after 22 hours exposure to different concentrations of nanoprobes (Figure 2A). However, after 2- and 3-days incubation, the cells appeared rounded and necrotic across all concentrations of nanoprobes (Figure 2B). For both MG-63 and Saos-2 cells there was a rapid induction of necrosis at the highest nanoprobe concentrations across days 1-3 (Figure 2C). Quantification of cell viability after 3 days confirmed Saos-2 cell numbers were reduced following exposure to *Vimentin* nanoprobes (Figure 2D) with viability apparently reducing with increasing nanoprobe concentration. MG-63 cells displayed enhanced resistant to the toxicity of the nanoprobes, with viability only reduced at the highest concentration (5 nM) examined.

Viability of Cells in Suspension was Reduced with Prolonged Incubation Time.

Human bone marrow cells are in suspension when exposed to nanoprobes and thus, to determine if cells in suspension were more vulnerable to cell toxicity than adherent cells. *Vimentin* nanoprobes were added to Saos-2 cells in suspension at 1 million cells per ml. Saos-2 cells were used given the increased sensitivity observed in comparison to MG-63 cells (Figure 2D). After 2-6 hours of contact time (2-6 hours), the Saos-2 cells were washed to remove the medium containing the nanoprobes, plated out and incubated. Figure 3A shows reduced cell viability at 48 hours, when Saos-2 cells were incubated with nanoprobes for only 4-6 hours. However, in the absence of nanoprobes the mean cell viability was also reduced suggesting reduced viability may be due to the incubation time rather than the nanoprobes.

Nanoprobe Concentration was Proportional to Detected Signal Intensity.

Low concentrations of *Vimentin* nanoprobes (0.1 nM and 0.2 nM) were explored to determine if reduced cell viability was related to high concentrations. After the specified contact time, 2-6 hours, the Saos-2 cells were washed and analysed by FACS for Cy5 fluorescence. With increasing nanoprobe contact time, the corresponding Cy5 signal detected in the Saos-2 cells was increased (Figure 4A, top panel), without any significant alteration in FAM signal (Figure 4A, lower panel). Although the intensity of the signal was increased, the ability to distinguish cells with a positive Cy5 signal from those without a Cy5 signal remained possible with 2 hours contact time at a 0.2 nM nanoprobe concentration (Figure 4B).

Negative Control Nanoprobe.

To determine if the nanoprobes were detecting their target mRNA, a nanoprobe containing a scrambled sequence that was not specific for any mRNA in the human genome database was designed (using BLASTn). Nanoprobes were added to human bone marrow cells for 2 hours at 0.2 nM final concentration. After washing, the cells were analysed by FACS. The scrambled nanoprobes produced a similar negative Cy5 signal as seen when no nanoprobes were added (Figure 5A, left hand images), whereas the *Vimentin* nanoprobes produced a positive Cy5 signal (Figure 5A, right hand image). While cells in the typical monocyte and granulocyte regions showed a distinct positive Cy5 signal with *Vimentin* nanoprobes, cells in the typical lymphocyte region produced a weaker, more diffuse signal (Figure 5B).

Nanoprobe Signal and mRNA Expression Levels are Qualitative.

Different concentrations of MG-63 cells were generated to provide a range of mRNA levels. The same volume of each cell concentration was used for RNA extraction and the cDNA (from the same volume of RNA solution) quantified by qPCR, or, plated into a qPCR plate, and nanoprobes specific for scrambled, *RUNX2*, or *Osteocalcin* added (0.2 nM) and incubated continuously at 37 °C with the Cy5 signal collected every 10 minutes for 15 hours. Figure 6A shows the Threshold (CT) values obtained for *RUNX2* and *Osteocalcin* qPCR with different concentrations of MG-63 cells indicating the differences in gene expression levels between cell concentrations and genes. The differences in gene expression were further highlighted when the relative expression levels of *RUNX2* and *Osteocalcin* were determined based on the equation $2^{-\text{CT Value}}$ (Figure 6B). The Cy5 signal detected for the different cell concentrations are indicated for the scrambled nanoprobe (Figure 6C and F), the *RUNX2* nanoprobe (Figure 6D and G), and *Osteocalcin* nanoprobe (Figure 6E and H). The scrambled nanoprobe produced no detectable Cy5 signal indicating the flare strand was not released from the sense strand. However, both *RUNX2* and *Osteocalcin* nanoprobes produced Cy5 signals indicating detection of specific mRNA. However, the Cy5 signals were not similar to the mRNA qPCR results (Figure 6B). Firstly, Overall *RUNX2* Cy5 signal (Figure 6D) was higher than the corresponding *Osteocalcin* Cy5 signal (Figure 6E), yet the opposite was observed for mRNA levels (Figure 6A and B). Secondly, relative mRNA levels for the different cell concentrations were not seen in the Cy5 signal levels e.g. 0.5×10^6 cells gave a higher Cy5 signal after 15 hours with *Osteocalcin* nanoprobe than 2×10^6 cells. Hence the Cy5 signal intensities were not related to absolute mRNA levels after 15 hours. In contrast, after around 2-3 hours, the Cy5 signal from the nanoprobes was more comparable with mRNA levels for both *RUNX2* (Figure 6G) and *Osteocalcin* (Figure 6H). However, the Cy5 signals intensity between the 2 genes was still not indicative of relative mRNA expression levels.

Optimisation of Nanoprobe Cellular Entry.

Commonly used antibody to enrich for human skeletal stem cells are Stro-1 [14] and Tra-1-60 [15]. The antigen for Stro-1 is the product of the HSPA8 gene [14] and for Tra-1-60 is a product of the podocalyxin gene [16]. We designed nanoprobes to target mRNA of these genes. This podocalyxin nanoprobe was observed to produce a strong Cy5 signal with human bone marrow stromal cells (Figure 7A). Even after 1-hour contact time, 60% of lymphocytes, and 100% of monocytes and granulocytes showed a Cy5 signal indicating that the nanoprobes were capable of producing a strong signal with only 1-hour contact time. Therefore, in our experiments, a 1-hour contact time was determined as better representation of the true Cy5 level than a 2-hour nanoprobe contact time.

Cy5 Signal was Maintained After 24 Hours at 4°C With 1 Hour Contact Time.

Human bone marrow cells were assessed for Cy5 expression from scrambled, *Vimentin*, and PODXL nanoprobes, following 1-hour contact time. After washing to remove the nanoprobes, the sample was divided with 50% of cells assessed by FACS immediately (Figure 7B, top panel), and the remaining 50% assessed by FACS after 24 hours incubation at 4°C (Figure 7B, bottom panel). There was negligible difference in the Cy5 signal detected at both timepoints, confirming the Cy5 signal is not lost following 24 hours incubation at 4°C.

Nanoprobes Showed Negligible Degradation Within Cells.

Representative FACS Cy5 versus FAM dot plots are shown (Figure 8) for human bone marrow samples used to isolate skeletal stem cells. The plots indicated very few of the nanoprobes showed DNA degradation as evidenced by FAM fluorescence. The FAM positive fluorescence detected was only found in combination with positive Cy5 fluorescence, suggesting the degradation occurred with or after Cy5 release. In addition, the proportion of FAM positive cells remained low, at 0.5-1.4%, even when the Cy5 positivity ranged 0.2-84.3%.

Different Nanoprobes Displayed Altered Abilities to Isolate Skeletal Stem Cells.

Nanoprobes targeting *HSPA8*, *PODXL*, *RUNX2*, *Osteocalcin*, or scrambled sequence were incubated with human bone marrow stromal cells for 1 hour at 0.2 nM final concentration. After washing, cells gated for single cells and monocytes were collected by FACS according to Cy5 fluorescence intensity with the positive fraction representing the highest 30% and negative being the lowest 30%. The recovered cells were subsequently incubated at 10,000 per well in 6 well plates for 14 days and cells stained to determine the number of colonies produced by colony-forming units-fibroblastic cells (CFU-F), which are indicative of skeletal stem cells (SSCs). Figure 9 shows that each nanoprobe produced varying levels of CFU-Fs, with *HSPA8*, *RUNX2*, and *Osteocalcin* nanoprobes producing significantly higher levels than *PODXL* and scrambled nanoprobes, with enrichment observed in comparison to unsorted cells. The gene specific nanoprobes showed negligible CFU-F formation from the nanoprobe Cy5 negative fraction. The scrambled nanoprobes showed CFU-F levels between unsorted cells and none in the highest 30% Cy5 positive cells, and intermediate CFU-F levels in the lowest 30% Cy5 negative cells. This confirms the scrambled nanoprobe was not specifically detecting CFU-F. Cells Isolated using the nanoprobes displayed a fibroblastic phenotype, as shown in Figure 10, with representative images of the cells within single CFU-F colonies isolated with the different nanoprobes.

Skeletal Stem Cells Resided Within the Brightest 10% of Cells, Regardless of Fluorescence Intensity.

Nanoprobes targeting different mRNAs were incubated with human bone marrow stromal cells for 1 hour at 0.2 nM final concentration as detailed above. After washing, cells were collected by FACS (gates on single cells and monocyte region on FSC v SSC plot) according to Cy5 fluorescence intensity. Cells were collected in the highest 60%, 30%, 20% or 10% fraction of fluorescent cells regardless of fluorescence intensity. Each set of collected cells was divided equally based on fluorescence intensity to provide a top and bottom fraction (Figure 11a). Cells in each fraction were then plated for CFU-F assay using 10,000 per well in 6 well plates for 14 days. For the top fraction, figure 11b shows that the 30% portion displayed increased CFU-F count compared to 60% portion, 20% portion displayed increased

CFU-F count compared to 30% portion, and 10% portion displayed increased CFU-F count compared to 20% portion. However, for the bottom fraction, CFU-F were only evident in the 10% portion indicating SSC were present and could be isolated in both the top and bottom fraction of the 10% portion. Thus, for maximum SSC enrichment the top fraction of the 10% portion should be collected, while, for maximum SSC recovery, the top fraction of the 20% portion should be collected.

Discussion

The current studies demonstrate optimisation of protocols and judicious oligonucleotide design/selection to facilitate the application of targeted detection of mRNA using oligonucleotide-coated gold nanoparticles in the isolation of human skeletal cell populations from human bone marrow stromal populations. We have previously shown the detection of mRNA using nanoprobes in live *Hydra* [17] and wound healing[18]. We have extended these studies and demonstrate the use of nanoprobes to now detect specific mRNA in human bone marrow stromal cells and importantly, the use of Cy5 signal to isolate human skeletal cells with minimal toxicity and an absence of nanoprobe degradation. Whereas we previously used a 3-hour contact time to detect mRNA in Hydra, we found that the flow cytometer was able to distinguish a Cy5 signal after only one-hour contact time of the cells with the nanoprobes. In addition, nanoprobes targeting different mRNAs showed altered abilities to detect stem cells, as evidenced by their ability to form colonies following culture.

A number of similar gold nanoprobe products suggest the application of contact times of 6 to 16 hours [19, 20]. The human osteoblast-like cell lines, MG-63 and Saos-2, used in the current study displayed excellent Cy5 signal after 22 hours contact time, and the cells remained healthy and viable. However, after 48 hours contact time the cells were observed to be rounded and necrotic. Hence, the number of nanoprobes per cell (which it is assumed increases over time), determined by nanoprobe concentration and contact time, the mRNA target of the nanoprobe (which may be inhibited by the nanoprobe), and the specific cell type, may be factors which all determine the toxicity of the nanoprobes or the Cy5 dye. Despite the observed cellular toxicity of the nanoprobes at high concentrations and long contact times, we were still able to detect nanoprobe Cy5 signals in cell lines after 9 days; with the cells in contact with the nanoprobes for 4 days until the first media change without nanoprobes. It is likely the cells were able to recover from any toxic effects of the nanoprobes following a change of media. However, it is unclear whether the nanoprobes were still present and producing a signal from mRNA, or if the nanoprobes were absent and the Cy5 dye remained in the cells. Following the addition of nanoprobes to human bone marrow stromal cells with 1-hour contact time, we were able to detect the same proportion and intensity of Cy5 signal in the cells immediately after washing, and after overnight incubation at 4 °C. This is likely a consequence of the inability of the flare strand to be released from the nanoprobe together with reduced mRNA activity.

Of the major cell types found in bone marrow, cells in the typical monocyte and granulocyte regions displayed good Cy5 signals from the different nanoprobes examined, whereas cells in the typical lymphocyte region showed reduced levels. This may be as a consequence of phagocytic uptake of the nanoprobes by monocytes and granulocytes. However, when the bone marrow cells were treated with 15 µM cytochalasin D to inhibit phagocytosis, no decrease in Cy5 signal was found (data not shown).
Interestingly, when we assessed the accumulation of Cy5 signal over a 15-hour period, we observed no correlation between the Cy5 signal and mRNA levels after 15 hours. This is in agreement with a study by Czarnek and Bereta [21], which showed Smartflare signal was not related to mRNA levels following overnight incubation with cells. However, we found that the nanoprobe signal correlated more strongly to mRNA levels, the shorter the exposure time to the nanoprobe of interest. These results may indicate the mRNA displaces the flare strand and subsequently unbinds from the sense strand. Thus, a single mRNA could displace flare strands from multiple nanoprobes. Furthermore, the longer the time between the addition of the nanoprobes and Cy5 detection, the higher the Cy5 signal from a single mRNA molecule and the higher the degree of discordance to true mRNA levels.

We used the PODXL nanoprobe as the uptake control in the current studies, to determine the one-hour contact time as this used the same chemistry as all other nanoprobes examined. The common uptake control is a directly labelled, extended length sense strand as this fluoresces at all times [21]. In the current studies, we observed negligible FAM fluorescence suggesting minimal DNA degradation of the nanoprobes. The level of FAM positivity remained low regardless of the level of Cy5 positivity within the sample, indicating the Cy5 signal was to mRNA binding rather than from DNA degradation.

Skeletal stem cells (SSCs) have the ability to generate colonies (termed colony-forming units-fibroblastic; CFU-F) when plated and cultured at limiting dilution [22]. The CFU-F assay harnesses this ability to identify potential skeletal stem cells and progenitor cells as each colony is derived from a single stem / early progenitor cell. Skeletal stem cells display upon CFU-F formation, a fibroblastic appearance when isolated and cultured. The colony appearance of CFUs isolated with the nanoprobes from the human bone marrow stromal samples at limiting dilution were observed to be fibroblastic supportive of SSC/early progenitor populations. Through the collection of different proportions of the brightest Cy5 cells with the different nanoprobes, regardless of their overall intensity, we were able to determine the CFU-Fs occurred in the top 10% of brightest cells. When this top 10% of brightest cells was divided equally into brightest and dimmest fractions, CFU-Fs were detected in both fractions. Hence, any further partitioning beyond the top 10% brightest cells would lead to loss of CFU-Fs. For the nanoprobes demonstrated here, nanoprobes targeting *HSPA8*, *RUNX2*, and *Osteocalcin* showed increased CFU-F enrichment compared to nanoprobes targeting *PODXL* or scrambled nanoprobes with no specific mRNA target.
In conclusion, the current studies illustrate the development and optimisation of protocols harnessing gold nanoparticles and judicious oligonucleotide selection to facilitate the application of targeted detection of mRNA in the isolation of select skeletal cell populations

from human bone marrow stromal populations with potential application across the cell biology arena and in biomedicine.

Acknowledgements

RO acknowledges support from the UK Regenerative Medicine Platform "Acellular / Smart Materials – 3D Architecture" (MR/R015651/1), the Rosetrees Trust, Wessex Medical Research. RO and AGK acknowledge financial support from the Biotechnology and Biological Sciences Research Council (BB/P017711/1).

References

1. Specht, E. A.; Braselmann, E.; Palmer, A. E., A Critical and Comparative Review of Fluorescent Tools for Live-Cell Imaging. *Annu. Rev. Physiol.* **2017,** *79*, 93-117.
2. Choi, C. H.; Hao, L.; Narayan, S. P.; Auyeung, E.; Mirkin, C. A., Mechanism for the endocytosis of spherical nucleic acid nanoparticle conjugates. *Proc. Natl. Acad. Sci. U. S. A.* **2013,** *110* (19), 7625-30.
3. Heuer-Jungemann, A.; El-Sagheer, A. H.; Lackie, P. M.; Brown, T.; Kanaras, A. G., Selective killing of cells triggered by their mRNA signature in the presence of smart nanoparticles. *Nanoscale* **2016,** *8* (38), 16857-16861.
4. Kang, K. A.; Wang, J.; Jasinski, J. B.; Achilefu, S., Fluorescence manipulation by gold nanoparticles: from complete quenching to extensive enhancement. *J Nanobiotechnology* **2011,** *9*, 16.
5. Heuer-Jungemann, A.; Harimech, P. K.; Brown, T.; Kanaras, A. G., Gold nanoparticles and fluorescently-labelled DNA as a platform for biological sensing. *Nanoscale* **2013,** *5* (20), 9503-10.
6. Chan, C. K. F.; Gulati, G. S.; Sinha, R.; Tompkins, J. V.; Lopez, M.; Carter, A. C.; Ransom, R. C.; Reinisch, A.; Wearda, T.; Murphy, M.; Brewer, R. E.; Koepke, L. S.; Marecic, O.; Manjunath, A.; Seo, E. Y.; Leavitt, T.; Lu, W.-J.; Nguyen, A.; Conley, S. D.; Salhotra, A.; Ambrosi, T. H.; Borrelli, M. R.; Siebel, T.; Chan, K.; Schallmoser, K.; Seita, J.; Sahoo, D.; Goodnough, H.; Bishop, J.; Gardner, M.; Majeti, R.; Wan, D. C.; Goodman, S.; Weissman, I. L.; Chang, H. Y.; Longaker, M. T., Identification of the Human Skeletal Stem Cell. *Cell* **2018,** *175* (1), 43-56.e21.
7. Sacchetti, B.; Funari, A.; Michienzi, S.; Di Cesare, S.; Piersanti, S.; Saggio, I.; Tagliafico, E.; Ferrari, S.; Robey, P. G.; Riminucci, M.; Bianco, P., Self-renewing osteoprogenitors in bone marrow sinusoids can organize a hematopoietic microenvironment. *Cell* **2007,** *131* (2), 324-36.
8. Mendez-Ferrer, S.; Michurina, T. V.; Ferraro, F.; Mazloom, A. R.; Macarthur, B. D.; Lira, S. A.; Scadden, D. T.; Ma'ayan, A.; Enikolopov, G. N.; Frenette, P. S., Mesenchymal and haematopoietic stem cells form a unique bone marrow niche. *Nature* **2010,** *466* (7308), 829-34.
9. Dawson, J. I.; Kanczler, J.; Tare, R.; Kassem, M.; Oreffo, R. O., Concise review: bridging the gap: bone regeneration using skeletal stem cell-based strategies - where are we now? *Stem Cells* **2014,** *32* (1), 35-44.
10. Black, C. R.; Goriainov, V.; Gibbs, D.; Kanczler, J.; Tare, R. S.; Oreffo, R. O., Bone Tissue Engineering. *Curr Mol Biol Rep* **2015,** *1* (3), 132-140.
11. Debnath, S.; Yallowitz, A. R.; McCormick, J.; Lalani, S.; Zhang, T.; Xu, R.; Li, N.; Liu, Y.; Yang, Y. S.; Eiseman, M.; Shim, J. H.; Hameed, M.; Healey, J. H.; Bostrom,

M. P.; Landau, D. A.; Greenblatt, M. B., Discovery of a periosteal stem cell mediating intramembranous bone formation. *Nature* **2018,** *562* (7725), 133-139.
12. Gothard, D.; Greenhough, J.; Ralph, E.; Oreffo, R. O., Prospective isolation of human bone marrow stromal cell subsets: A comparative study between Stro-1-, CD146- and CD105-enriched populations. *J Tissue Eng* **2014,** *5*, 2041731414551763.
13. Kyriazi, M.-E.; Giust, D.; El-Sagheer, A. H.; Lackie, P. M.; Muskens, O. L.; Brown, T.; Kanaras, A. G., Multiplexed mRNA Sensing and Combinatorial-Targeted Drug Delivery Using DNA-Gold Nanoparticle Dimers. *ACS Nano* **2018,** *12* (4), 3333-3340.
14. Fitter, S.; Gronthos, S.; Ooi, S. S.; Zannettino, A. C., The Mesenchymal Precursor Cell Marker Antibody STRO-1 Binds to Cell Surface Heat Shock Cognate 70. *Stem Cells* **2017,** *35* (4), 940-951.
15. Guillot, P. V.; Gotherstrom, C.; Chan, J.; Kurata, H.; Fisk, N. M., Human first-trimester fetal MSC express pluripotency markers and grow faster and have longer telomeres than adult MSC. *Stem Cells* **2007,** *25* (3), 646-54.
16. Schopperle, W. M.; DeWolf, W. C., The TRA-1-60 and TRA-1-81 human pluripotent stem cell markers are expressed on podocalyxin in embryonal carcinoma. *Stem Cells* **2007,** *25* (3), 723-30.
17. Moros, M.; Kyriazi, M. E.; El-Sagheer, A. H.; Brown, T.; Tortiglione, C.; Kanaras, A. G., DNA-Coated Gold Nanoparticles for the Detection of mRNA in Live Hydra Vulgaris Animals. *ACS applied materials & interfaces* **2019,** *11* (15), 13905-13911.
18. Vilela, P.; Heuer-Jungemann, A.; El-Sagheer, A.; Brown, T.; Muskens, O. L.; Smyth, N. R.; Kanaras, A. G., Sensing of Vimentin mRNA in 2D and 3D Models of Wounded Skin Using DNA-Coated Gold Nanoparticles. *Small* **2018,** *14* (12), e1703489.
19. Seferos, D. S.; Giljohann, D. A.; Hill, H. D.; Prigodich, A. E.; Mirkin, C. A., Nano-flares: probes for transfection and mRNA detection in living cells. *J. Am. Chem. Soc.* **2007,** *129* (50), 15477-15479.
20. McClellan, S.; Slamecka, J.; Howze, P.; Thompson, L.; Finan, M.; Rocconi, R.; Owen, L., mRNA detection in living cells: A next generation cancer stem cell identification technique. *Methods* **2015,** *82*, 47-54.
21. Czarnek, M.; Bereta, J., SmartFlares fail to reflect their target transcripts levels. *Sci. Rep.* **2017,** *7* (1), 11682.
22. Friedenstein, A. J.; Chailakhyan, R. K.; Latsinik, N. V.; Panasyuk, A. F.; Keiliss-Borok, I. V., Stromal cells responsible for transferring the microenvironment of the hemopoietic tissues. Cloning in vitro and retransplantation in vivo. *Transplantation* **1974,** *17* (4), 331-40.

Table 1. Nanoprobe sequences

Nanoprobe Target	Sense Strand Sequence	Flare Strand Sequence
Scrambled	ATGGTATACCGAAAGACTGTTAAAAA	AACAGTCTTTCG
HSPA8	AGCAGTACGGAGGCGTCTTACA	TGTAAGACGCCTC
Osteocalcin	TGATGGAGGGTGAGCCACAATC	GATTGTGGCTCACC
Podocalyxin	TGGAGGTTGCAACTGTAGTGGT	ACCACTACAGTTG
RUNX2	AGATCGTTGAACCTTGCTACTT	AAGTAGCAAGGTT
Vimentin	CTTTGCTCGAATGTGCGGACTT	AAGTCCGCACA

Table 2. qPCR Primer sequences

mRNA Target	Forward Sequence	Reverse Sequence
RUNX2	GTAGATGGACCTCGGGAACC	GAGGCGGTCAGAGAACAAAC
Osteocalcin	GGCAGCGAGGTAGTGAAGAG	CTCACACACCTCCCTCCT

Figure 1.
Vimentin-targeting nanoprobes were added to the adherent human osteoblast-like cell lines MG-63 and Saos-2 at 0.2 nM, 1 nM, and 6.25 nM final concentrations. Control cells had equivalent volume of PBS added. Cells were incubated for 9 days with a media change without nanoprobes after 4 and 7 days. A). Composite image showing bright field and Cy5 (red) images. B). Composite image showing bright field and FAM (green) images. Bar represents 100µm.

Figure 2.
Vimentin-targeting nanoprobes were added to the adherent human osteoblast-like cell lines MG-63 and Saos-2 at the different final concentrations shown. RealTime-Glo Annexin V Apoptosis and Necrosis Assay reagents were added at day 0. A). Composite image showing bright field and Cy5 (red) images after 22 hours exposure to nanoprobes. Bar represents 50µm. B). Composite image of MG-63 (top panel) and Saos-2 cells (bottom panel) showing bright field, Cy5 (red), and necrotic cell (green) images after 2- and 3-days incubation with nanoprobes. Bar represents 50 µm. C). Apoptosis index (top panel), necrosis index (bottom panel), and viability (bottom panel) of cells, with added nanoprobes, for days 1-3. Graphs show means with 95% confidence limits. *** $p<0.001$, ** $p<0.01$, * $p<0.05$. n=3 for each bar.

Figure 3.
Vimentin-targeting nanoprobes added at 0.1 nM or 0.2 nM final concentration to Saos-2 cells in suspension at 1 million cells per ml. After the specified contact time (2-6 hours), the cells were washed to remove medium containing the nanoprobes, plated out and cell viability assessed after 48 hours. Graph show means with 95% confidence limits. * $p<0.05$. n=3 for each bar.

Figure 4.
A). *Vimentin*-targeting nanoprobes added at 0.1 nM or 0.2 nM final concentration to Saos-2 cells in suspension at 1 million cells per ml. After the specified contact time (2-6 hours), the cells were washed and analysed by flow cytometry for Cy5 (top row) and FAM (bottom row) fluorescence intensity. B). Percentage of positive Cy5 cells determined by flow cytometry with different nanoprobe concentrations and contact times.

Figure 5.
Vimentin-targeting and scrambled nanoprobes added to human bone marrow cells for 2 hours at 0.2 nM final concentration. After washing, the cells were analysed by flow cytometry for Cy5 fluorescence intensity. Selection criteria for the different cell fraction regions (Top panels). Cy5 intensity overlay plots for the different nanoprobes for whole bone marrow (Bottom panel, outer left) and different cell fraction regions.

Figure 6.
Different concentrations of MG-63 cells generated and the same volume of each cell concentration was either used for RNA extraction and then the cDNA quantified by qPCR, or plated into a qPCR plate, nanoprobes specific for scrambled, RUNX2, or Osteocalcin added (at final concentration of 0.2 nM) and incubated continuously at 37 °C with the Cy5 signal collected every 10 minutes for 15 hours (C, D, and E). A). Relative expression levels of *RUNX2* and *Osteocalcin* based on value $2^{-CT\ Value}$ for different cell concentrations. n=3 for each bar. Cy5 signal detected for different cell concentrations using scrambled (B), RUNX2 (C) and osteocalcin (E) nanoprobes after 15 hours. Cy5 signal detected for different cell

concentrations using RUNX2 (D) and osteocalcin (F) nanoprobes after 5 hours. Graphs show mean with 95% confidence limits. n=3 for each cell concentration.

Figure 7.
A). *Podocalyxin*-targeting or scrambled nanoprobes added to human bone marrow cells for 1, 2 or 3 hours at 0.2 nM final concentration. After washing, the cells were analysed by flow cytometry for Cy5 fluorescence intensity. Cy5 intensity overlay plots for the different nanoprobes for different cell types within the bone marrow as determined by forward and side scatter characteristics. Colours shown are no nanoprobes (red), scrambled nanoprobe (yellow), *Podocalyxin* (green). B). *Podocalyxin*-targeting, *Vimentin*-targeting, or scrambled nanoprobe were added to human bone marrow cells for 1 hour at 0.2 nM final concentration. After washing to remove the nanoprobes, the sample was divided with 50% of cells assessed by flow cytometry immediately (top panel), the remaining 50% of the samples was assessed by flow cytometry after 24 hours incubation at 4°C (bottom panel). Cy5 intensity overlay plots for the different nanoprobes for different cell types within the bone marrow as determined by forward and side scatter characteristics. Colours shown are scrambled nanoprobe (red), *Vimentin* nanoprobe (yellow), and *Podocalyxin* nanoprobe (green).

Figure 8.
Nanoprobes targeting *HSPA8*, *Podocalyxin (PODXL)*, *RUNX2*, *Osteocalcin*, or scrambled sequence were incubated with human bone marrow cells for 1 hour at 0.2 nM final concentration. After washing, cells were gated for single cells and monocytes were collected by FACS. Representative dot plots are shown for Cy5 fluorescence versus FAM fluorescence for each nanoprobe.

Figure 9.
Nanoprobes targeting *HSPA8*, *Podocalyxin (PODXL)*, *RUNX2*, *Osteocalcin*, or scrambled sequence were incubated with human bone marrow cells for 1 hour at 0.2 nM final concentration. After washing, cells were gated for single cells and cells in the typical monocyte region were collected by FACS according to Cy5 fluorescence intensity with positive being the highest 30% and negative being the lowest 30%. The recovered cells were incubated at 10,000 per well in 6 well plates for 14 days. The cells were subsequently stained to determine the number of CFU-F colonies. Graph shows CFU-F count for each nanoprobe as a percentage of the CFU-F number from unselected cells which were plated to give the equivalent of 10,000 cells in the monocyte region per well. Graphs show means with 95% confidence limits. n=2-3 patients for each nanoprobe. For Cy5 positive data only: *** $p<0.001$ and ** $p<0.01$.

Figure 10.
Nanoprobes targeting *HSPA8*, *Podocalyxin (PODXL)*, *RUNX2*, *Osteocalcin*, or scrambled sequence were incubated with human bone marrow cells for 1 hour at 0.2 nM final concentration. After washing, cells gated for single cells and monocytes were collected by FACS according to Cy5 fluorescence intensity with positive being the highest 30% and negative being the lowest 30%. The recovered cells were subsequently incubated at 10,000 per well in 6 well plates for 14 days. The cells were stained to determine the number of CFU-F colonies. Representative images of cells within individual colonies isolated with each nanoprobe are shown. Bar represents 200µm. Insets show individual colonies in 6-well plate.

Figure 11.

Nanoprobes including those targeting *HSPA8*, *Podocalyxin (PODXL)*, *RUNX2*, *Osteocalcin*, and scrambled sequence were incubated with human bone marrow cells for 1 hour at 0.2 nM final concentration. After washing, cells were gated for single cells and cells in the monocyte region were collected by FACS according to Cy5 fluorescence intensity. A). The brightest 60%, 30%, 20% or 10% of fluorescent cells were collected. Each set of collected cells was divided equally based on fluorescence intensity to give top and bottom fractions. The recovered cells were then incubated at 10,000 per well in 6 well plates for 14 days to determine the number of CFU-F colonies. B). CFU-F counts from different bone marrow samples incubated with different nanoprobes according to cells isolated from either the top or bottom fraction of the collected cells: brightest 60% (black), brightest 30% (red), brightest 20% (green) or brightest 10% (purple). Data from 26 patient samples.

Figure 1.

A.

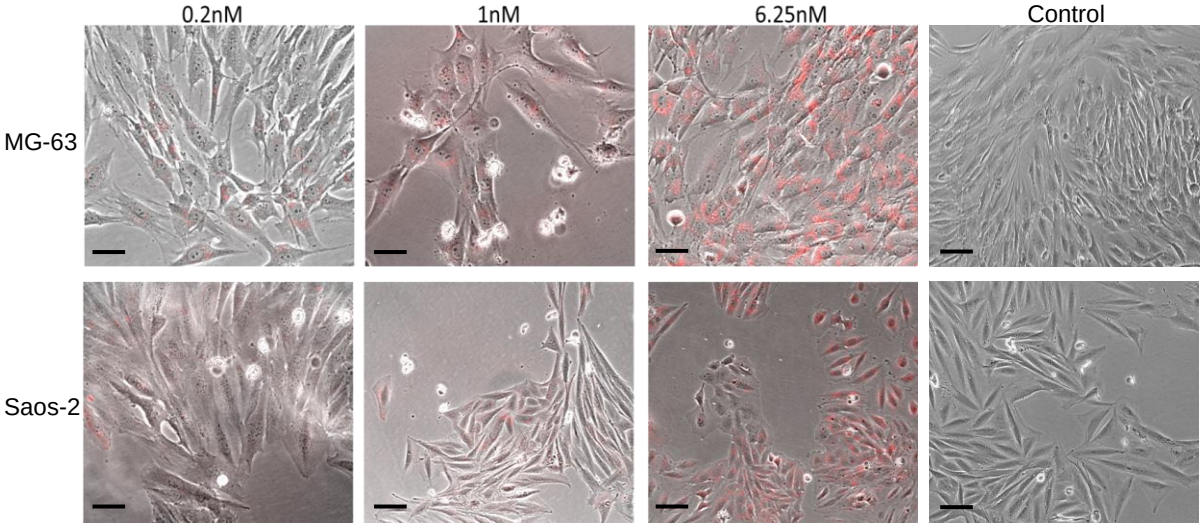

B.

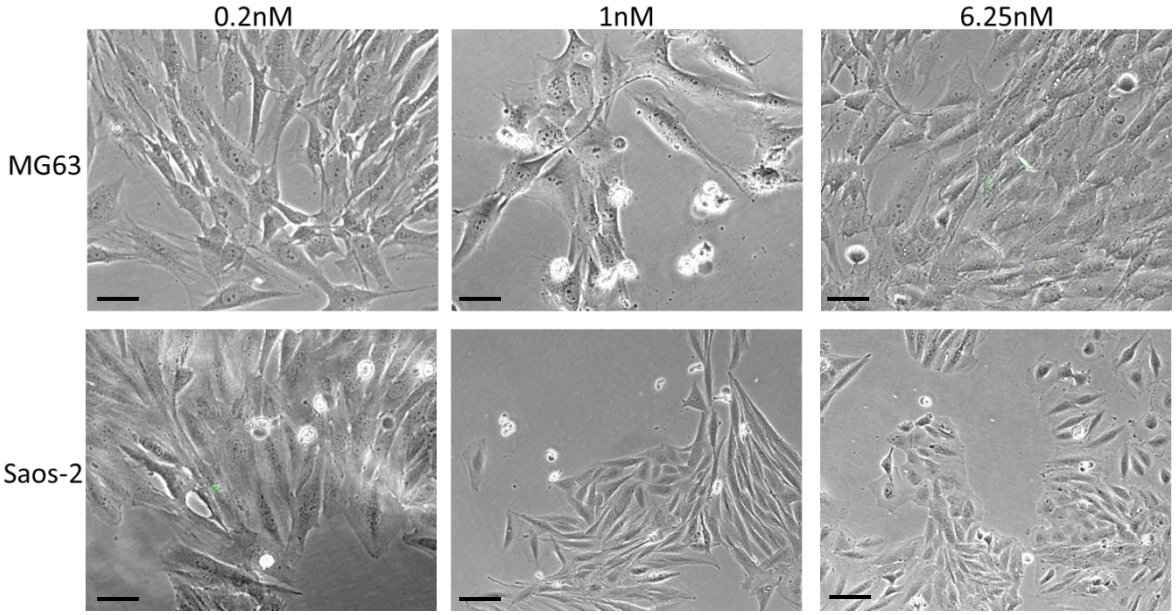

Figure 2.

A.

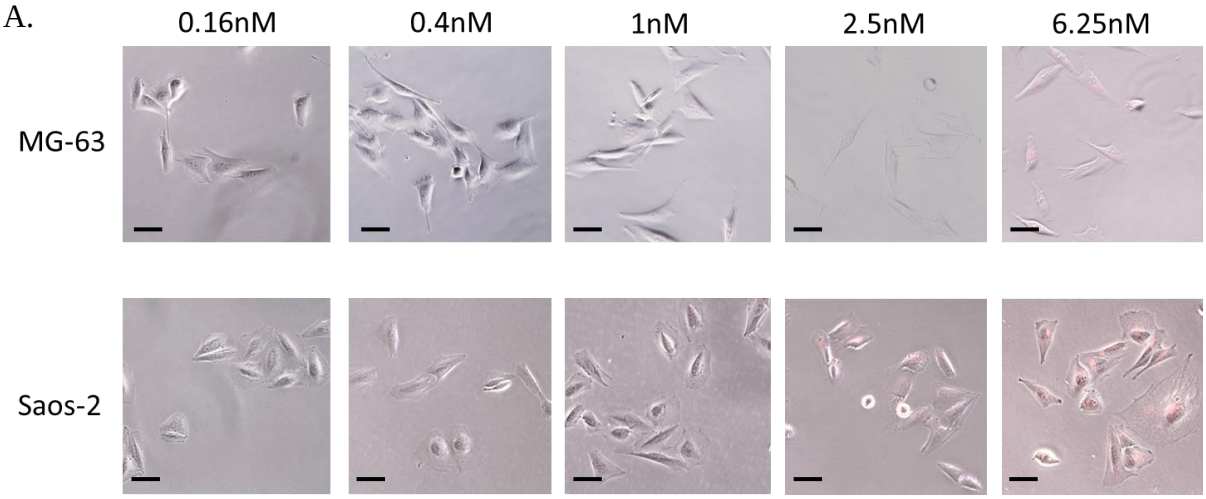
0.16nM
0.4nM
1nM
2.5nM
6.25nM
MG-63
Saos-2

B.

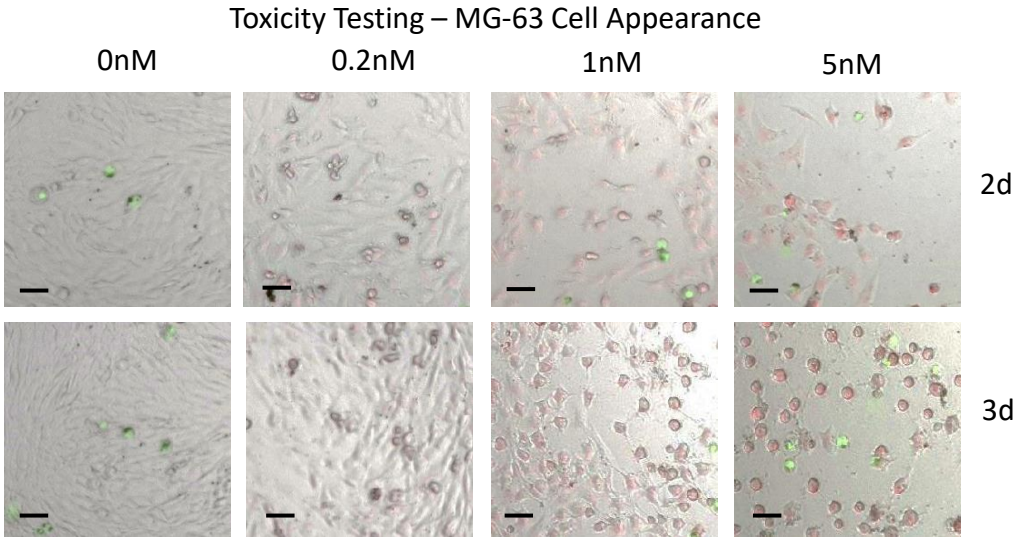
Toxicity Testing – MG-63 Cell Appearance
0nM
0.2nM
1nM
5nM
2d
3d

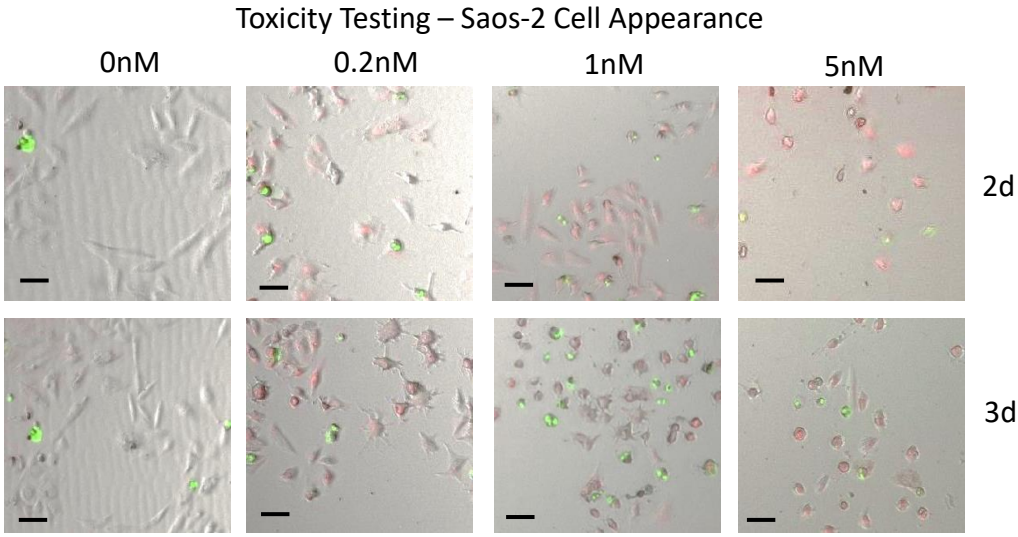
Toxicity Testing – Saos-2 Cell Appearance
0nM
0.2nM
1nM
5nM
2d
3d

C.

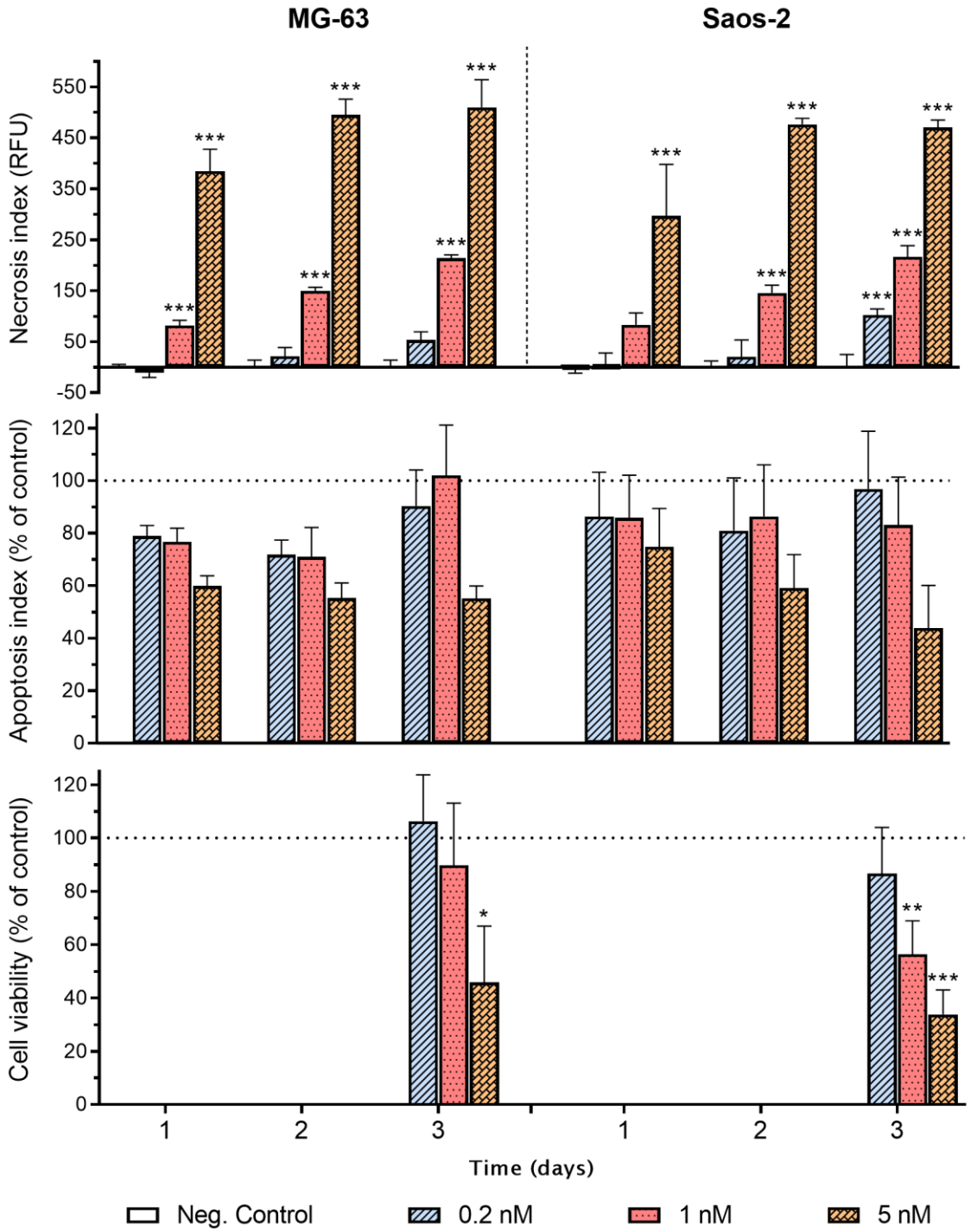
MG-63
Saos-2
Necrosis index (RFU)
Apoptosis index (% of control)
Cell viability (% of control)
Time (days)
Neg. Control
0.2 nM
1 nM
5 nM

Figure 3.

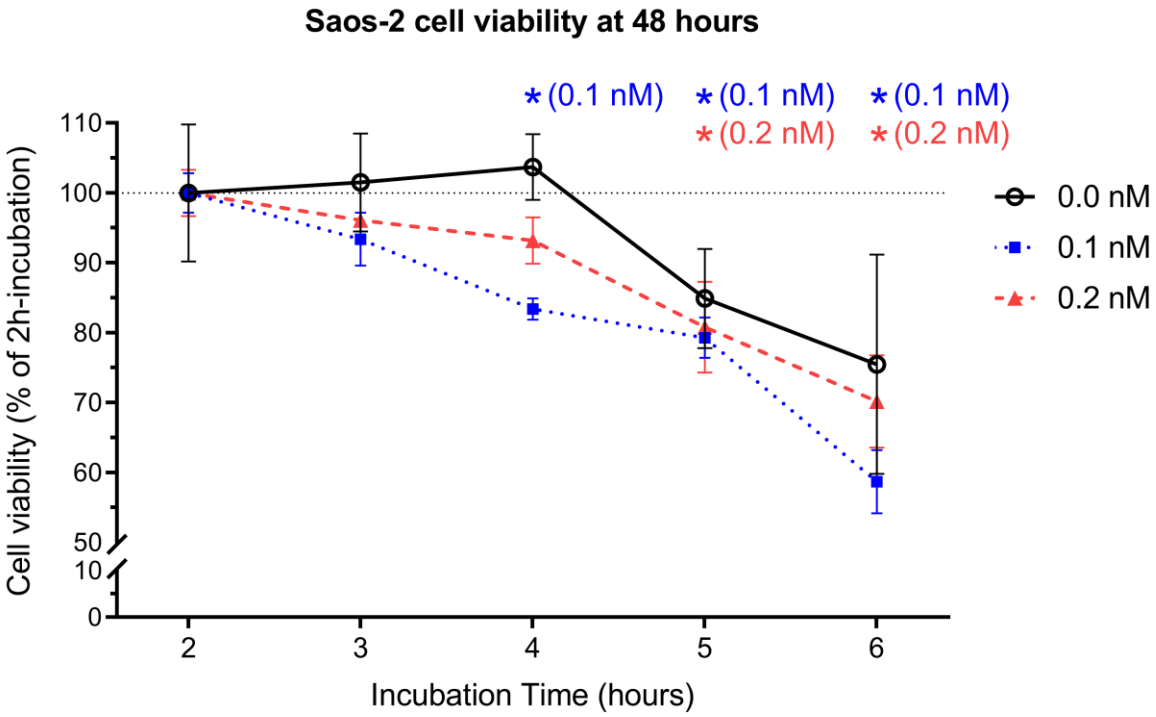
Saos-2 cell viability at 48 hours
*(0.1 nM)
*(0.1 nM)
*(0.1 nM)
*(0.2 nM)
*(0.2 nM)
Cell viability (% of 2h-incubation)
110
100
90
80
70
60
50
10
0
2
3
4
5
6
Incubation Time (hours)
0.0 nM
0.1 nM
0.2 nM

Figure 4.

A.

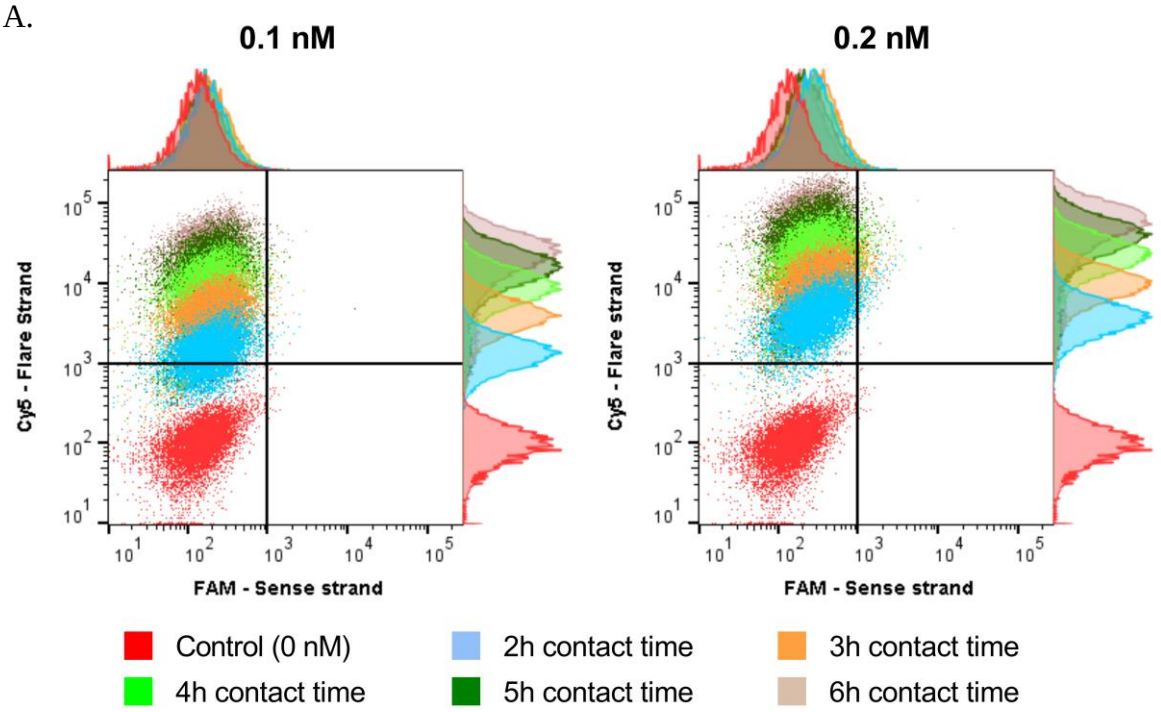
0.1 nM
0.2 nM
Cy5 - Flare Strand
Cy5 - Flare strand
FAM - Sense strand
Control (0 nM)
2h contact time
3h contact time
4h contact time
5h contact time
6h contact time

B.

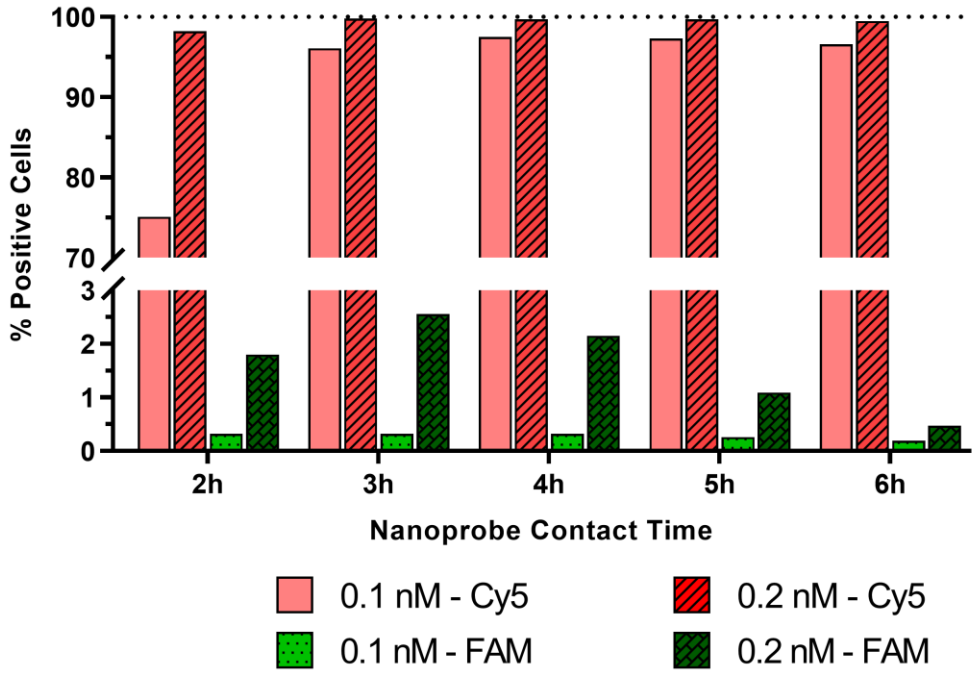
% Positive Cells
100
90
80
70
3
2
1
0
2h
3h
4h
5h
6h
Nanoprobe Contact Time
0.1 nM - Cy5
0.2 nM - Cy5
0.1 nM - FAM
0.2 nM - FAM

Figure 5.

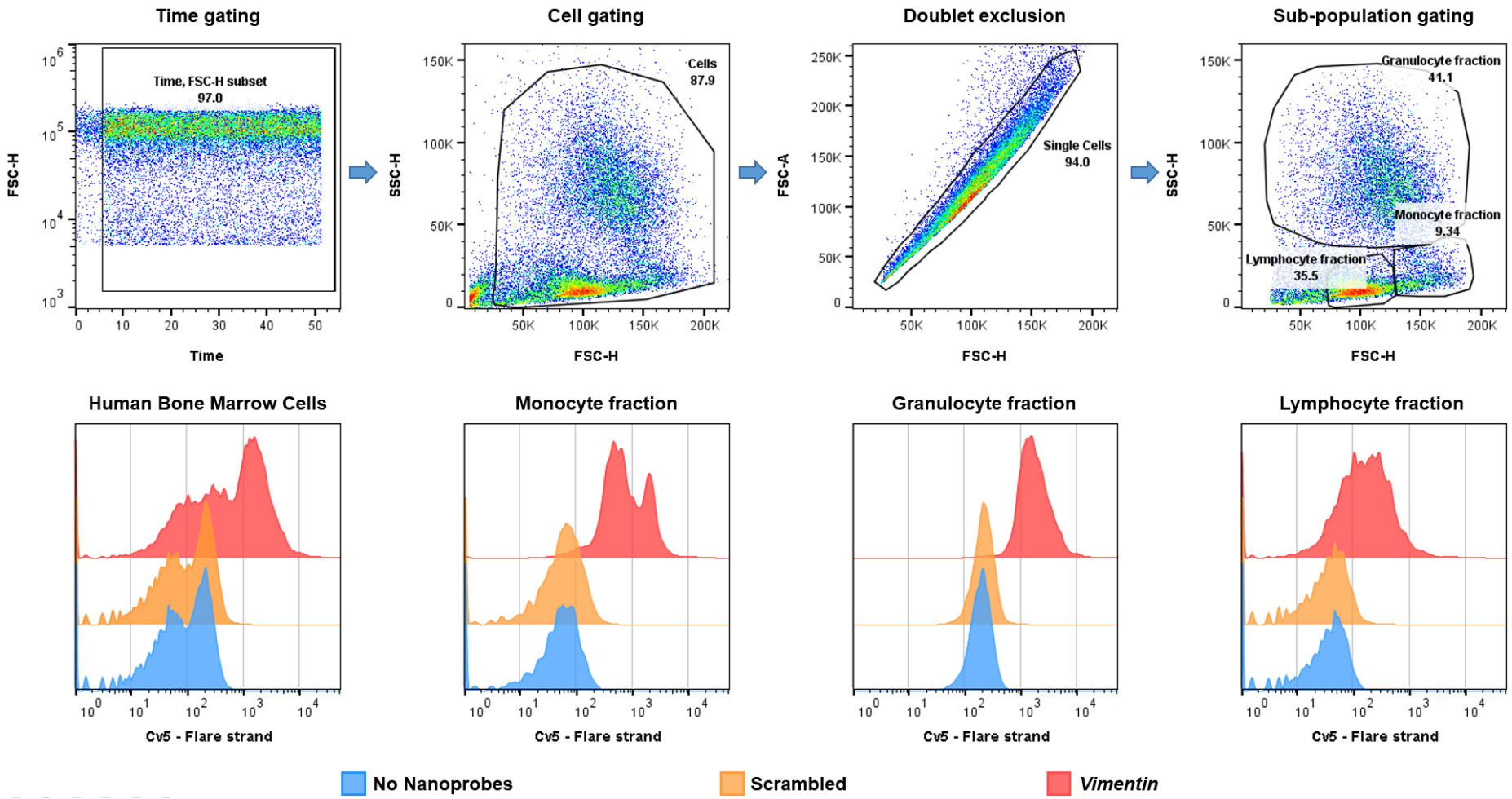
Time gating
Time, FSC-H subset
97.0
FSC-H
Time
Cell gating
Cells
87.9
SSC-H
FSC-H
Doublet exclusion
Single Cells
94.0
FSC-A
FSC-H
Sub-population gating
Granulocyte fraction
41.1
Monocyte fraction
9.34
Lymphocyte fraction
35.5
SSC-H
FSC-H
Human Bone Marrow Cells
Monocyte fraction
Granulocyte fraction
Lymphocyte fraction
Cv5 - Flare strand
No Nanoprobes
Scrambled
Vimentin

Figure 6.

A.

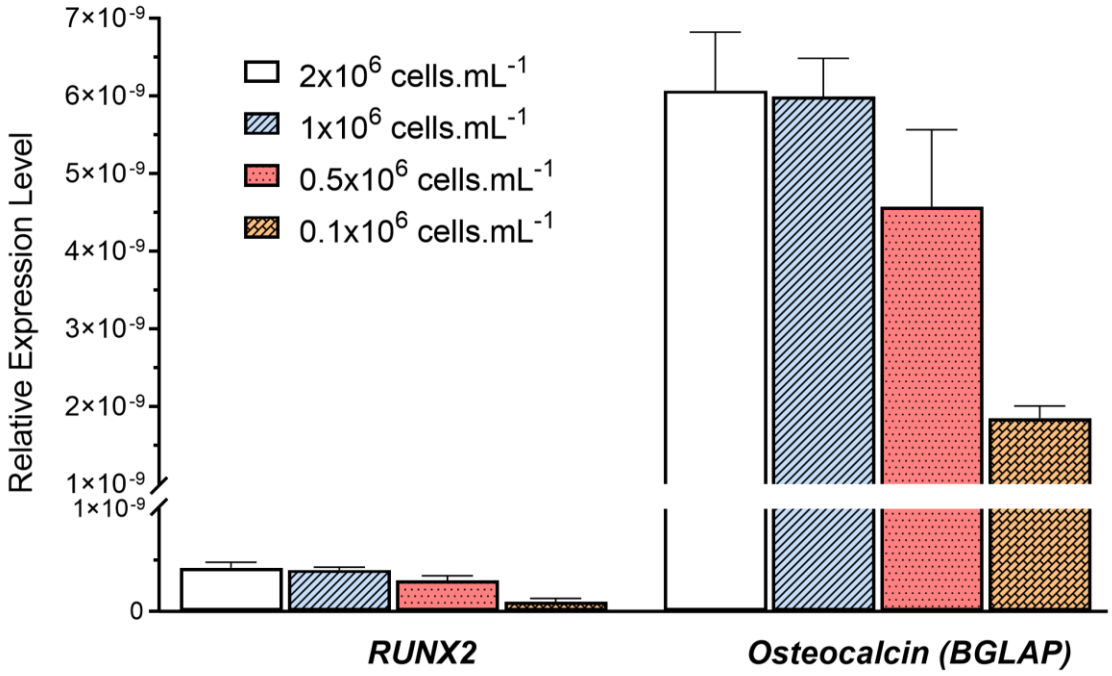
Relative Expression Level
7×10-9
6×10-9
5×10-9
4×10-9
3×10-9
2×10-9
1×10-9
1×10-9
0
2x10^6 cells.mL^-1
1x10^6 cells.mL^-1
0.5x10^6 cells.mL^-1
0.1x10^6 cells.mL^-1
RUNX2
Osteocalcin (BGLAP)

B.

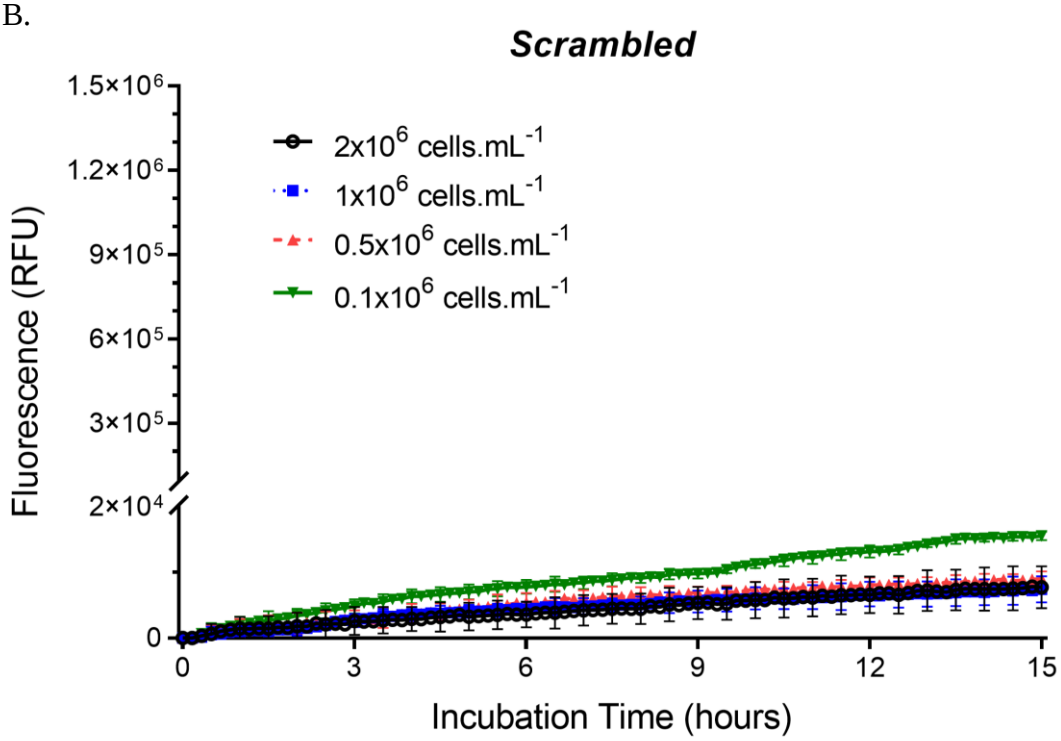
Scrambled
Fluorescence (RFU)
1.5×10^6
1.2×10^6
9×10^5
6×10^5
3×10^5
2×10^4
0
2x10^6 cells.mL^-1
1x10^6 cells.mL^-1
0.5x10^6 cells.mL^-1
0.1x10^6 cells.mL^-1
0
3
6
9
12
15
Incubation Time (hours)

C.

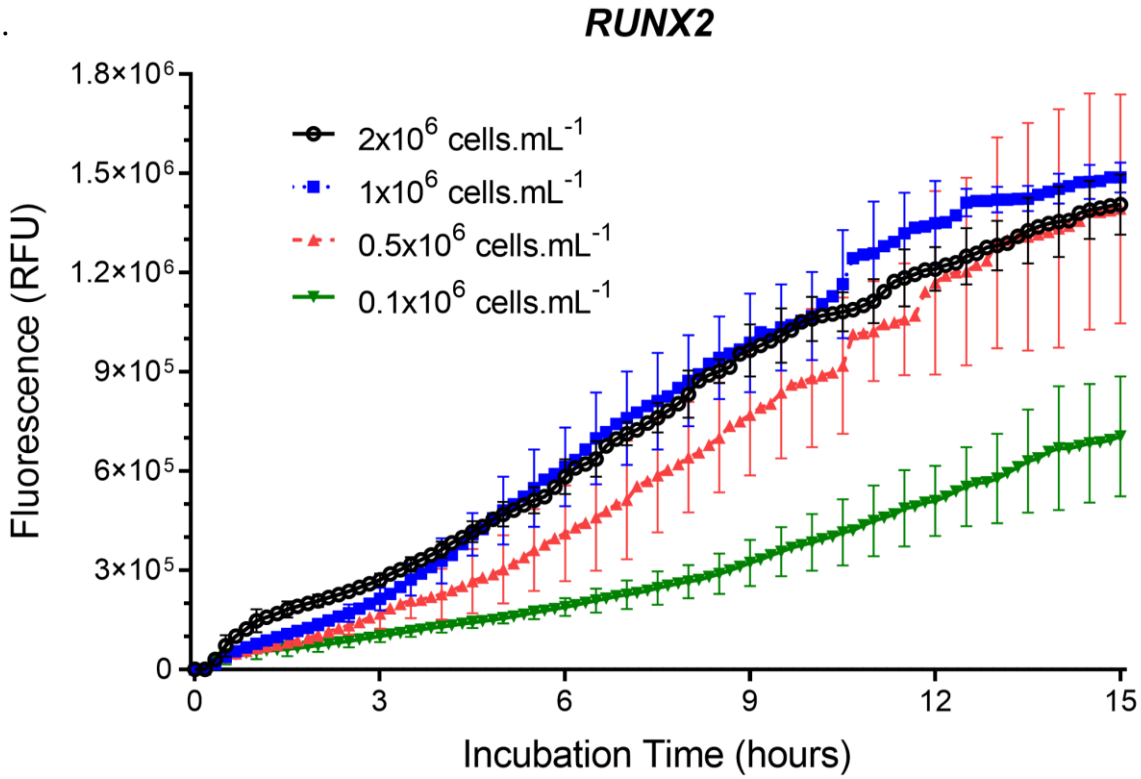
RUNX2
1.8×10⁶
1.5×10⁶
1.2×10⁶
9×10⁵
6×10⁵
3×10⁵
0
Fluorescence (RFU)
2x10⁶ cells.mL⁻¹
1x10⁶ cells.mL⁻¹
0.5x10⁶ cells.mL⁻¹
0.1x10⁶ cells.mL⁻¹
0
3
6
9
12
15
Incubation Time (hours)

D.

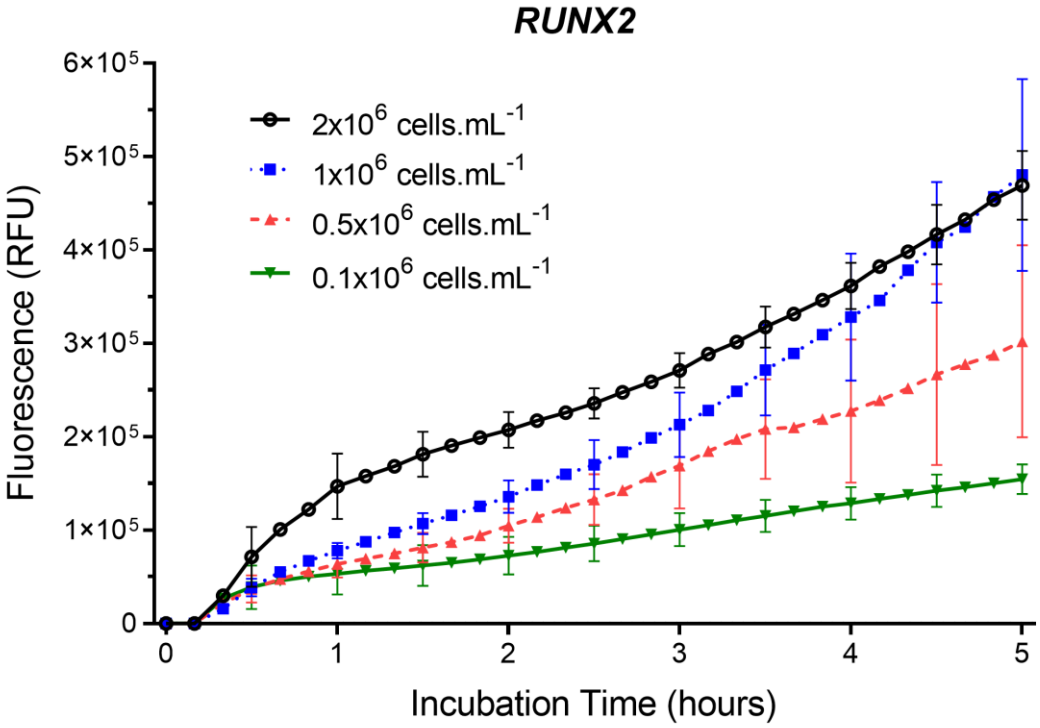
RUNX2
6×10⁵
5×10⁵
4×10⁵
3×10⁵
2×10⁵
1×10⁵
0
Fluorescence (RFU)
2x10⁶ cells.mL⁻¹
1x10⁶ cells.mL⁻¹
0.5x10⁶ cells.mL⁻¹
0.1x10⁶ cells.mL⁻¹
0
1
2
3
4
5
Incubation Time (hours)

E.

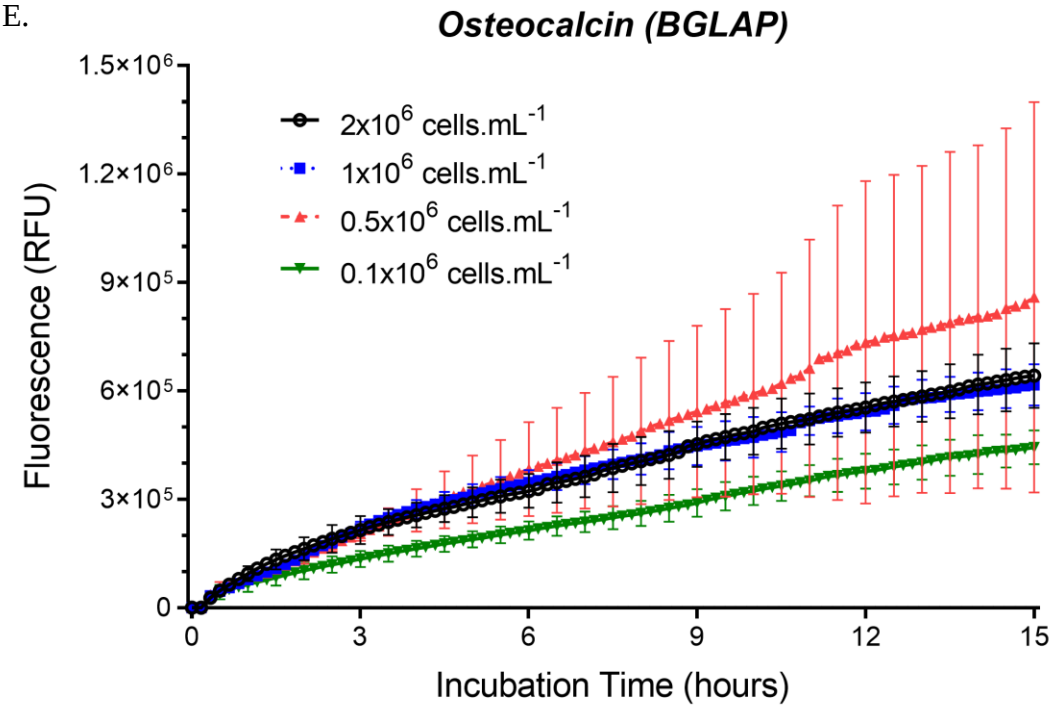
Osteocalcin (BGLAP)
1.5×10⁶
1.2×10⁶
9×10⁵
6×10⁵
3×10⁵
0
Fluorescence (RFU)
2x10⁶ cells.mL⁻¹
1x10⁶ cells.mL⁻¹
0.5x10⁶ cells.mL⁻¹
0.1x10⁶ cells.mL⁻¹
0
3
6
9
12
15
Incubation Time (hours)

F.

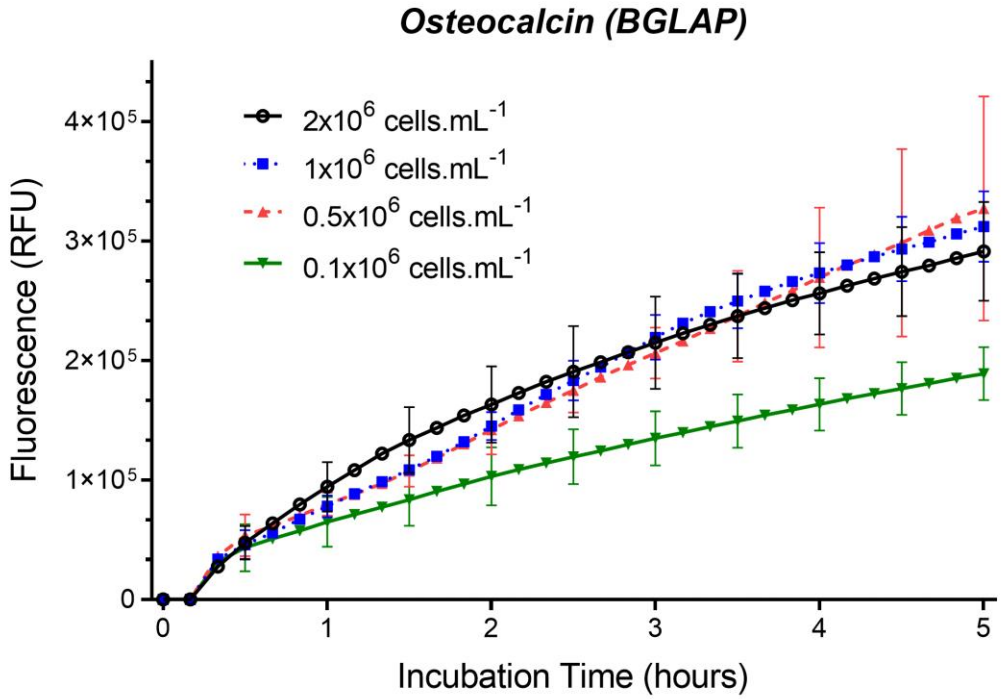
Osteocalcin (BGLAP)
4×10⁵
3×10⁵
2×10⁵
1×10⁵
0
Fluorescence (RFU)
2x10⁶ cells.mL⁻¹
1x10⁶ cells.mL⁻¹
0.5x10⁶ cells.mL⁻¹
0.1x10⁶ cells.mL⁻¹
0
1
2
3
4
5
Incubation Time (hours)

Figure 7.

A.

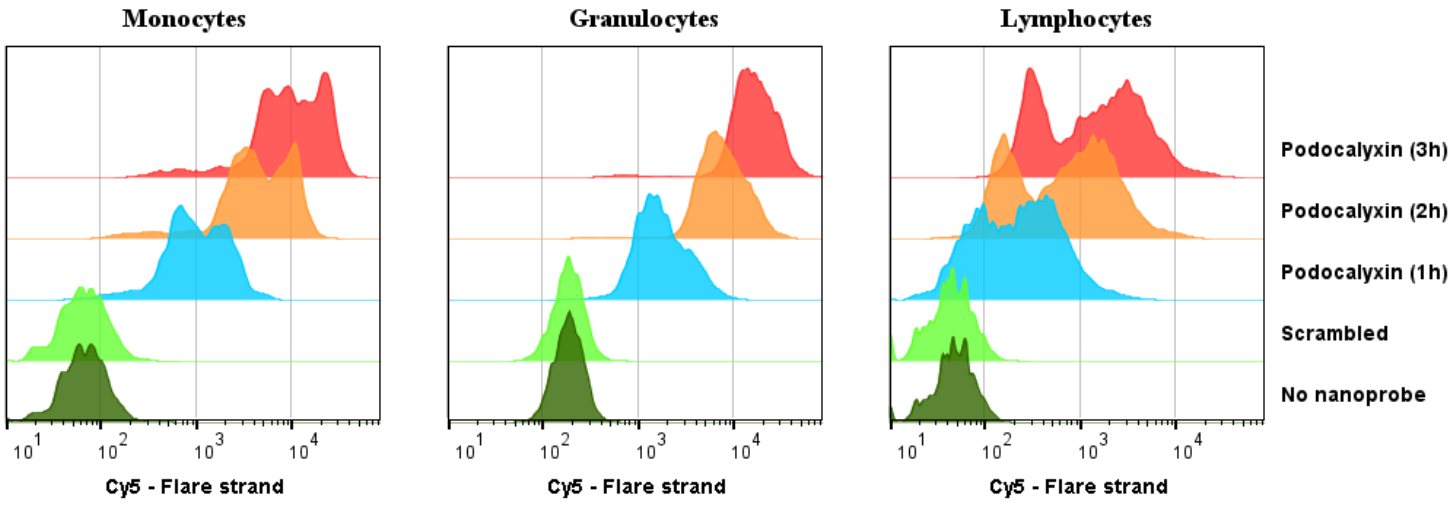
Monocytes
Granulocytes
Lymphocytes
Podocalyxin (3h)
Podocalyxin (2h)
Podocalyxin (1h)
Scrambled
No nanoprobe
10^1 10^2 10^3 10^4
Cy5 - Flare strand

B.

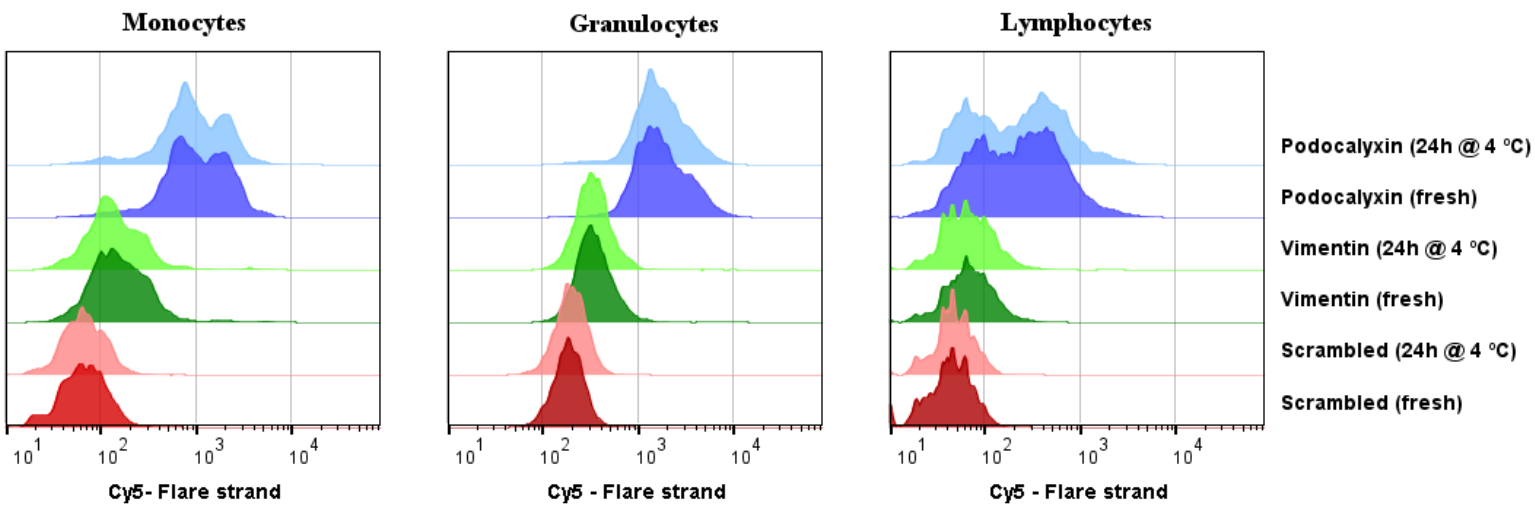
Monocytes
Granulocytes
Lymphocytes
Podocalyxin (24h @ 4 °C)
Podocalyxin (fresh)
Vimentin (24h @ 4 °C)
Vimentin (fresh)
Scrambled (24h @ 4 °C)
Scrambled (fresh)
10^1 10^2 10^3 10^4
Cy5- Flare strand
Cy5 - Flare strand
Cy5 - Flare strand

Figure 8.

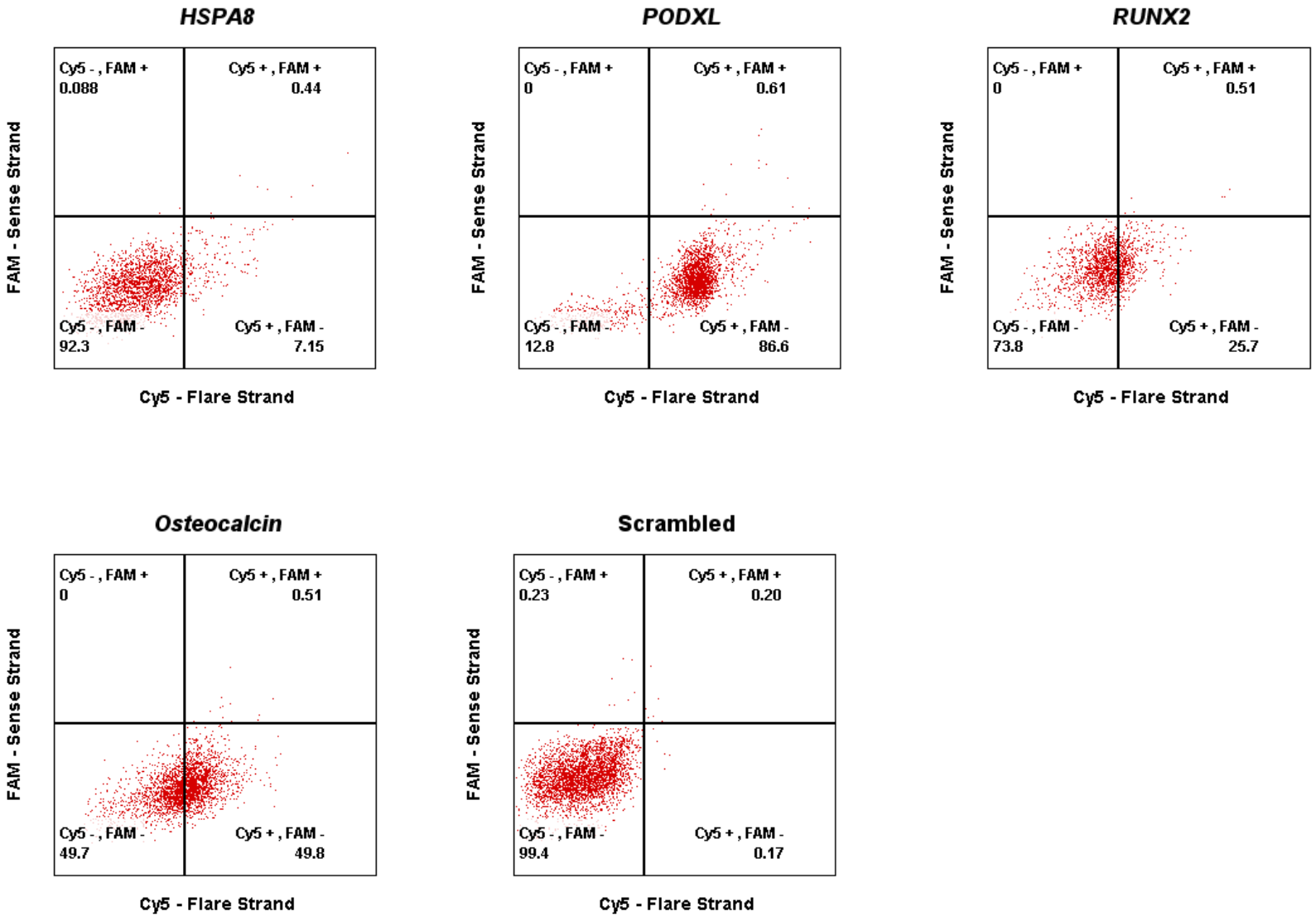
HSPA8
Cy5 - , FAM +
0.088
Cy5 + , FAM +
0.44
Cy5 - , FAM -
92.3
Cy5 + , FAM -
7.15
FAM - Sense Strand
Cy5 - Flare Strand
PODXL
Cy5 - , FAM +
0
Cy5 + , FAM +
0.61
Cy5 - , FAM -
12.8
Cy5 + , FAM -
86.6
FAM - Sense Strand
Cy5 - Flare Strand
RUNX2
Cy5 - , FAM +
0
Cy5 + , FAM +
0.51
Cy5 - , FAM -
73.8
Cy5 + , FAM -
25.7
FAM - Sense Strand
Cy5 - Flare Strand
Osteocalcin
Cy5 - , FAM +
0
Cy5 + , FAM +
0.51
Cy5 - , FAM -
49.7
Cy5 + , FAM -
49.8
FAM - Sense Strand
Cy5 - Flare Strand
Scrambled
Cy5 - , FAM +
0.23
Cy5 + , FAM +
0.20
Cy5 - , FAM -
99.4
Cy5 + , FAM -
0.17
FAM - Sense Strand
Cy5 - Flare Strand

Figure 9.

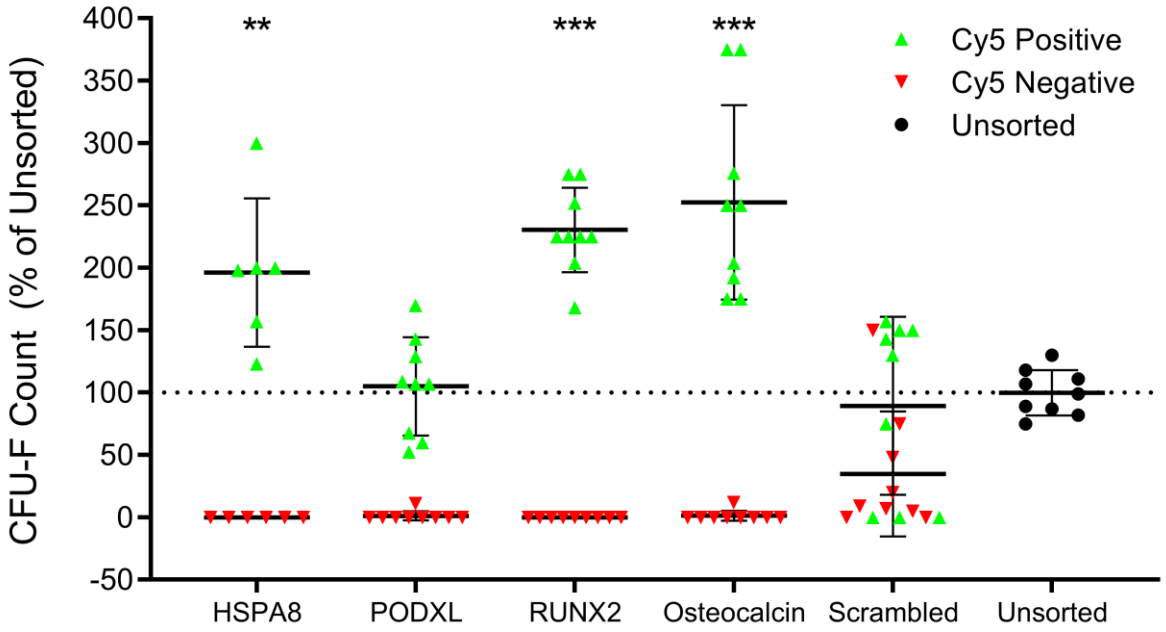
CFU-F Count (% of Unsorted)
400
350
300
250
200
150
100
50
0
-50
**
***
***
Cy5 Positive
Cy5 Negative
Unsorted
HSPA8
PODXL
RUNX2
Osteocalcin
Scrambled
Unsorted

Figure 10.

HSPA8 nanoprobe, Cy5 Positive

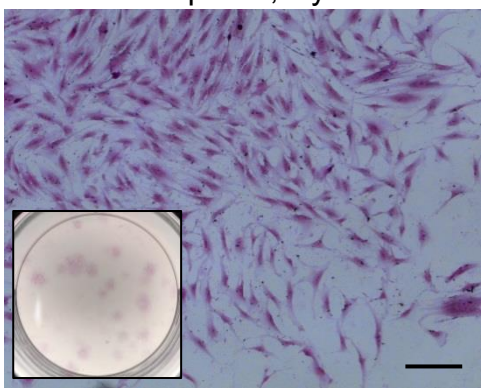

Osteocalcin nanoprobe, Cy5 Positive

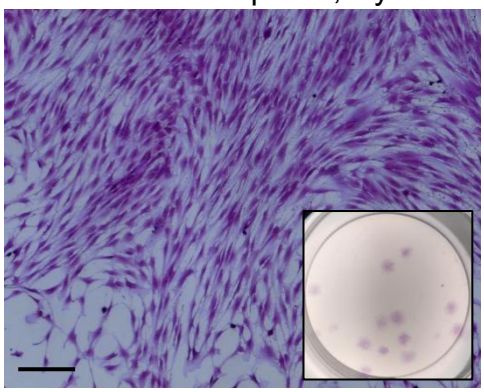

PODXL nanoprobe, Cy5 Positive

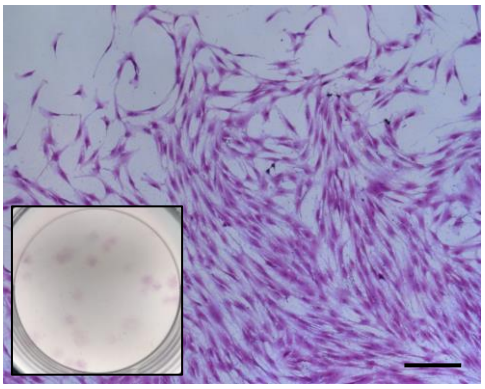

RUNX2 nanoprobe, Cy5 Positive

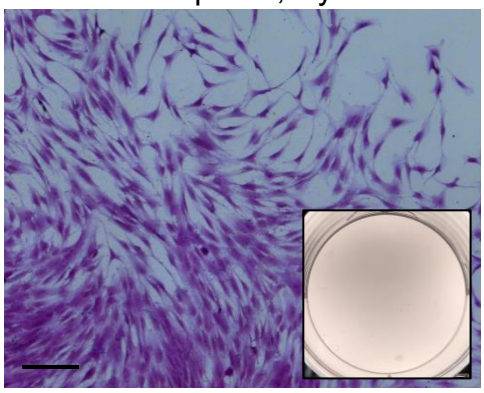

Scrambled nanoprobe, Cy5 Positive

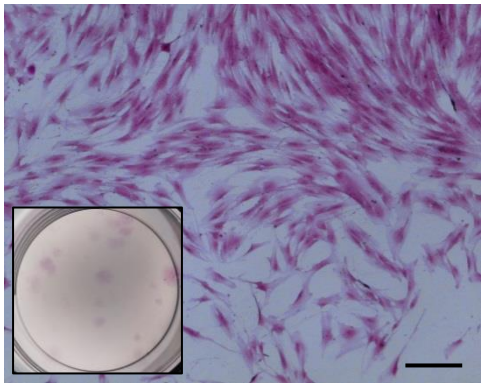

Scrambled nanoprobe, Cy5 Negative

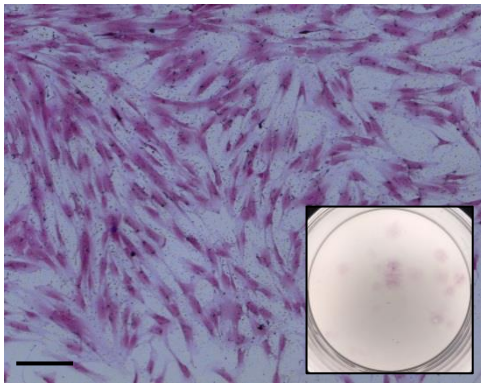

Unsorted Cells

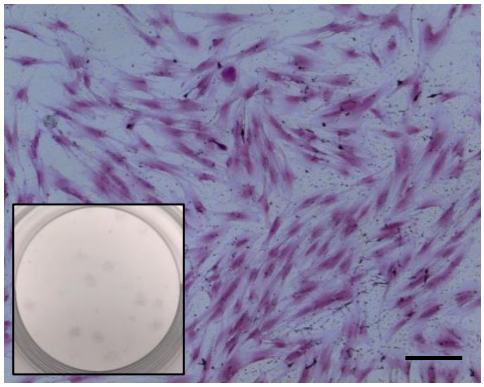

Figure 11.

A.

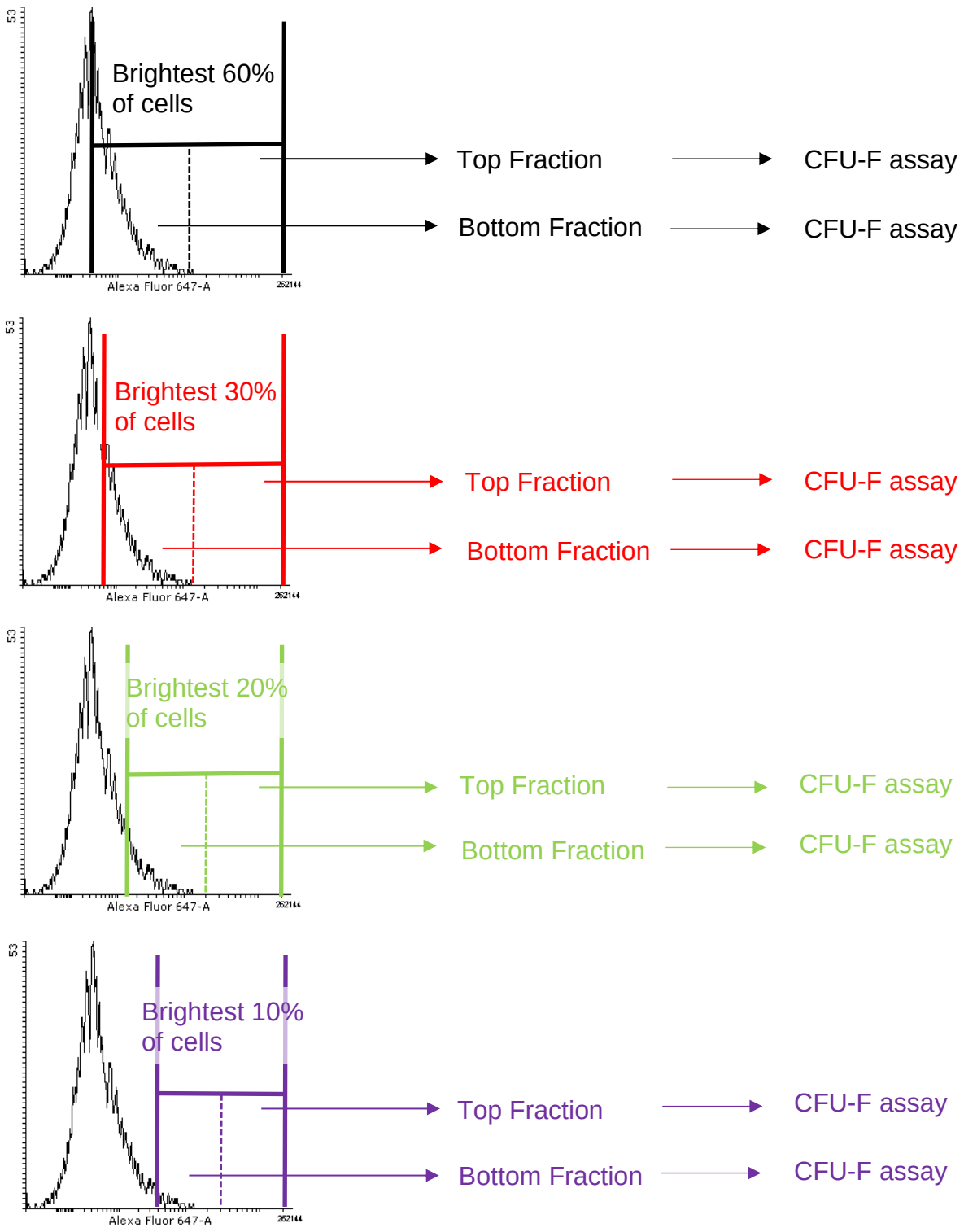
53
Brightest 60%
of cells
Alexa Fluor 647-A
262144
Top Fraction
CFU-F assay
Bottom Fraction
CFU-F assay
53
Brightest 30%
of cells
Alexa Fluor 647-A
262144
Top Fraction
CFU-F assay
Bottom Fraction
CFU-F assay
53
Brightest 20%
of cells
Alexa Fluor 647-A
262144
Top Fraction
CFU-F assay
Bottom Fraction
CFU-F assay
53
Brightest 10%
of cells
Alexa Fluor 647-A
262144
Top Fraction
CFU-F assay
Bottom Fraction
CFU-F assay

B.

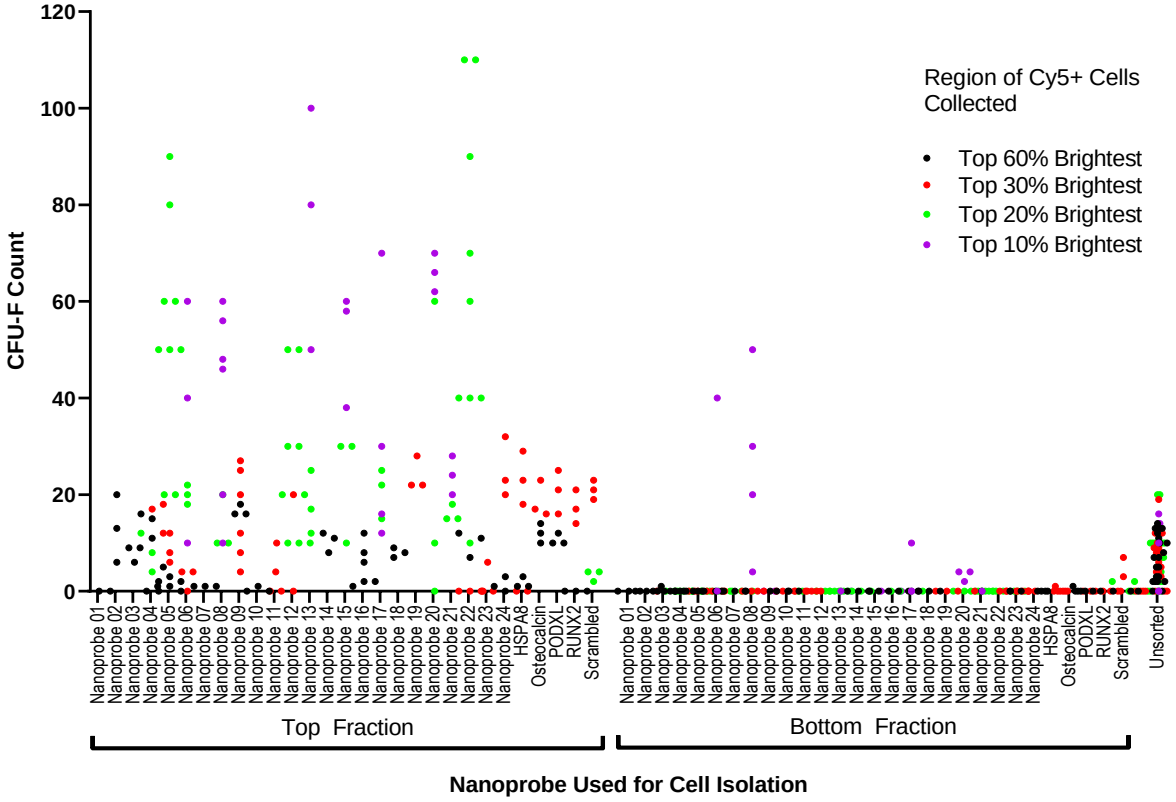
CFU-F Count
120
100
80
60
40
20
0
Region of Cy5+ Cells Collected
Top 60% Brightest
Top 30% Brightest
Top 20% Brightest
Top 10% Brightest
Nanoprobe 01
Nanoprobe 02
Nanoprobe 03
Nanoprobe 04
Nanoprobe 05
Nanoprobe 06
Nanoprobe 07
Nanoprobe 08
Nanoprobe 09
Nanoprobe 10
Nanoprobe 11
Nanoprobe 12
Nanoprobe 13
Nanoprobe 14
Nanoprobe 15
Nanoprobe 16
Nanoprobe 17
Nanoprobe 18
Nanoprobe 19
Nanoprobe 20
Nanoprobe 21
Nanoprobe 22
Nanoprobe 23
Nanoprobe 24
HSPA8
Osteocalcin
PODXL
RUNX2
Scrambled
Unsorted
Top Fraction
Bottom Fraction
Nanoprobe Used for Cell Isolation